EFFECT OF SURFACE CHEMICAL MODIFICATION ON HYDROPHILICITY, PROTEIN ADSORPTION AND PLATELET ADHESION

Carla Sofia Nogueira Rodrigues Teixeira

Tese submetida à Faculdade de Engenharia do Porto para candidatura à obtenção de grau de Mestre em Engenharia Biomédica

Faculdade de Engenharia

Universidade do Porto

2004

This thesis was supervised by:

Professor Mário Adolfo Barbosa

Faculdade de Engenharia, Universidade do Porto

Dr. Maria Cristina L. Martins

INEB-Instituto de Engenharia Biomédica, Laboratório de Biomateriais

The host intitution of this thesis was:

INEB-Instituto de Engenharia Biomédica, Laboratório de Biomateriais

Universidade do Porto, Portugal

The research described in this thesis was financially supported by:

European project: Novel intervertebral Disc Prostheses (nº G5RD-CT-2000-00267)

…to Hugo

"To obtain Knowledge, add things everyday; to get Wisdom, delete things everyday"

Chinese philosopher Lao Tsu

Acknowledgements

This thesis has been a process of self-discovery and I have quite a number of people to thank for it.

Firstly, I would like to express a deep sense of gratitude, esteem and affection towards my supervisor Prof. Mário Barbosa, for his criticism, suggestions and inspiration. Your time and effort in guiding me along this long road are greatly appreciated. I wish to sincerely thank for your support, excellent conditions and working environment at the Laboratory.

I wish to express my warmest thanks to my co-supervisor Dr. Cristina Martins, for valuable ideas, advice and trust in me during this research. Your enthusiasm sustained my research through disappointments and difficulties. You have helped immensely in clarifying many points. Thanks for all the support and friendship.

I also would like to acknowledge the collaboration of several persons from the following institutions:

Centro de Materiais da Universidade do Porto (CEMUP)- Dr. Carlos Sá for his help and availability during the X-ray Photoelectron (XPS) and Scanning Electron Microscopy (SEM) analysis and Daniela Silva for the assistance on SEM.

Institute of Composite and Biomedical Materials (ICBM), National Research Council and Interdisciplinary Research Centre in Biomaterials, University of Naples 'Federico II'- Professor Luigi Ambrosio for his availability, Dr. Filippo Causa and António Gloria for the helpful discussions about composites and their mechanical behaviour.

Instituto da Investigação da Floresta e Papel RAÍZ - Dr. Fernanda Paula Furtado for the availability in ozonation treatments and Sousa Pinto for the technical support.

Instituto de Engenharia Mecânica e Gestão Industrial (INEGI) – Professor Torres Marques for the availability, Eng. José Esteves for the helpful discussions and for sharing his expertise in tensile strength tests and and Paulo Nóvoa for the technical assistance.

Instituto Superior de Engenharia do Porto ISEP- Professor Mário Carvalho and Eng. Paulo Silva for the support in the UV treatments.

Instituto Português do Sangue IPS- Drª Marília Morais and Drª Salomé Maia for the availability, Ana Sofia Oliveira and Raquel Pacheco for technical support.

I wish to thank Alexandre Salvador for the assistance in flow citometry analysis and Drª Paula Sampaio for the assistance with the fluorescence microscope.

I would like to express my gratitude to Pedro Granja who supported me through many valuable discussions and invested a lot of time to share his knowledge with me. Thank you for reading over and over my drafts!!

I am very thankful to Professor Fernando Jorge Monteiro, Ana Queiroz and Inês Gonçalves (my angel…) for all the scientific discussions, advices, encouragement and friendship. I am grateful to Sandra Teixeira for all the support and friendship, Manuela Brás for technical support and for the "ten minutes". Add to this Ana Paula Filipe, our secretary, whom I will thank as a representative of all those people I bothered repeatedly and was rewarded only by their kindness and generosity. Thank you to all!!!

I would like to especially thank my parents, family and friends for their love and support. Especially to my father, who had provided critical feedback during the writing of this thesis, but even though I still love you!

This thesis is dedicated to my husband, Hugo, for his cherished and constant support of me throughout my graduate career. Thank you for your patience and understanding, for your inspiration and support, and for always being there for me. Your love and presence in my life has given me strength and determination in such a way that only you would know. I couldn't have made this far without you by my side. I love you!!

International Conference Proceedings Books

Rodrigues Teixeira S, Ferreira L, Granja PL, Barbosa MA. Composite hydrogels as Intervertebral Disc Substitutes – Wettability studies and mechanical characterization of PHEMA hydrogels reinforced with ozonated bundles of PET fibers. BioÉvora2004 - XXVII Symposium of the SIB. Évora, Portugal, Sept 9-11, 2004. p. O19.

Ferreira L, **Rodrigues Teixeira S**, Evangelista MB, Barbosa MA. Composite hydrogels as Intervertebral Disc Substitutes - I. Surface ozonation of poly (ethylene Terephthalate) fibers to improve their adhesion to PHEMA hydrogels. BioÉvora2004 - XXVII Symposium of the SIB. Évora, Portugal, Sept 9-11, 2004. p. O12.

Rodrigues Teixeira S, Granja PL, Barbosa MA. PHEMA hydrogels reinforced with modified PET fibers for biomedical applications. 18th European Conference on Biomaterials. Stuttgart, Germany, October 1-4, 2003.

Abstract

One relevant aspect of surface modifications of biomaterial applications resides in the alteration of chemical and physical properties of the surface maintaining an adequate mechanical behaviour. In this context, surface modifications can be used to improve the compatibility of a material with the surrounding tissue as well as the interactions between two different materials.

The present work is composed of two parts. The first part concerned the effect of surface wettability on protein adsorption and on platelet adhesion, using model surfaces. The second part was carried out in the framework of the European project “Novel Intervertebral Disc Prostheses” and consists in developing a composite between the hydrophobic poly (ethylene terephtalate) (PET) and the hydrophilic poly (hydroxylethyl methacrylate) (PHEMA) by enhancing the interaction between these two polymers through surface modification of PET.

When in direct contact with blood biomaterials are prone to induce the formation of clots if platelets and proteins related with the blood coagulation system are activated,. The effect of surface wettability on the adsorption of the plasma protein human fibrinogen (HFG), as well as platelet adhesion, was investigated using self-assembled monolayers (SAMs). In order to achieve a range of surfaces with different wettabilities and exposed functional groups, SAMs were prepared with different percentages of hydrophobic (-CH_3, C15CH_3) and hydrophilic functional groups (-OH, C11OH). Ellipsometry and contact angle measurements were used to characterize these surfaces. The thickness and the contact angle of this SAMs decreased linearly as the concentration of C11OH increased. Fibrinogen adsorption also decreased linearly as the hydrophilicity of the surface increased (increase of the C11OH concentration), as

detected by quantifying the radiolabelled protein. The mixed SAMs with 65% of the C11OH showed considerable HFG adsorption, when adsorption studies were performed using a pure HFG solution. However, when albumin (HSA) was present as a competitive protein, in a ratio HSA/HFG similar to that found in blood, these SAMs showed lower HFG affinity. In addition, HFG pre-adsorbed on these SAMs could be more easily exchanged by albumin in solution than by fibrinogen. Although the most hydrophilic SAMs (100% C11OH) showed the lowest HFG adsorption, competitive studies demonstrated that this surface had the highest HFG affinity when other proteins were present in solution. Scanning Electron Microscopy (SEM) micrographs showed that platelet adhesion was absent for 65% C11OH SAMs. In the case of the other SAMs tested, the results showed an increase in platelet adhesion as the methyl (hydrophobic) groups on the surface increased. Platelet adhesion was also high on gold. The hydrophobic $C15CH_3$ SAM was highly platelet reactive because the shape of the adhered platelet was mostly in spread dendritic and spread forms, as observed by SEM.

A composite material based on a PHEMA hydrogel matrix reinforced with PET fibers modified by ozonation was developed in view of their application as a intervertebral disc substitute. The results showed a dramatic decrease of the contact angle, from 74º to unmodified PET to 38° after 6h of ozonation treatment in specific conditions. The effect of PET's hydrophilicity on its adhesion to PHEMA was then characterized by tensile strength tests, and by analyses of the fracture surface's morphology by SEM. The adhesion between PET and PHEMA was thus improved, as shown by tensile strength tests. SEM micrographs confirmed that the best adhesion between treated PET fiber and PHEMA hydrogel matrix was obtained when PET fibers were treated with ozone for 6 hours and immediately immersed in a PHEMA reactive solution.

Resumo

Um dos aspectos relevantes da modificação de superfícies na aplicação de biomateriais reside na alteração das propriedades químicas e físicas da superfície mantendo um comportamento mecânico adequado. Neste contexto, a modificação de superfícies pode ser usada para melhorar a compatibilidade de um material com os tecidos circundantes bem como para melhorar as interacções entre os dois materiais distintos.

O presente trabalho é composto por duas partes. A primeira parte está relacionada com o efeito da molhabilidade da superfície na adsorpção de proteínas e na adesão de plaquetas, utilizando superfícies modelo. A segunda parte foi realizada no âmbito do Projecto Europeu *Novel Intervertebral Disc Prostheses*, que consiste no desenvolvimento de um compósito entre o poli (etileno tereftalato) (PET) -hidrofóbico- e o poli (2-hidroxietil metacrilato) (PHEMA) -hidrofílico- através do incremento da interacção entre od dois polímeros por modificação superficial do PET.

Quando em contacto directo com o sangue os biomateriais podem induzir a formação de coágulos se as plaquetas e as proteínas relacionadas com o sistema de coagulação forem activadas. O efeito da molhabilidade da superfície na adsorpção da proteína sanguínea fibrinogénio (HFG) e na adesão de plaquetas foi estudado usando monocamadas auto-estruturadas (SAMs). De modo a obter superfícies com uma gama de molhabilidades diversas e de grupos funcionais expostos, as SAMs foram preparadas com diferentes percentagens de grupos funcionais hidrofóbicos (-CH_3, C15CH3) e hidrofílicos (-OH, C11OH). Utilizaram-se a elipsometria e a medição de ângulos de contacto foram usadas para caracterizar estas superfícies. A espessura e os ângulos de contacto destas superfícies decresceram linearmente com o aumento da concentração de C11OH. A adsorção de fibrinogénio também decresceu linearmente com o aumento da

hidrofilicidade superficial (aumento da concentração de C11OH), tal como determinado por quantificação da proteína marcada radioactivamente. As SAMs mistas (65% C11OH) apresentaram uma adsorção de HFG considerável nos estudos de adsorção realizados com solução pura de HFG. Contudo, quando a albumina (HSA) estava presente como proteína de competição, numa razão HSA/HFG semelhante aquela encontrada no sangue, estas SAMs apresentaram uma afinidade para o fibrinogénio inferior. Para além disso, o HFG pré-adsorvido nestas SAMs foi mais facilmente trocado pela albumina em solução do que pelo fibrinogénio. Embora as SAMs com mais grau de hidrofilicidade (100% de C11OH) tenham apresentado a mais baixa adsorção de HFG, os estudos de competição demonstraram que esta superfície apresentou a afinidade com o HFG mais elevada quando outras proteínas estavam presentes. As fotomicrografias obtidas por microscopia electrónica de varrimento (SEM) demonstraram que adesão de plaquetas foi nula em SAMs com 65% de C11OH. No caso das restantes SAMs ensaiadas, os resultados indicaram um aumento da adesão de plaquetas com o aumento de grupos metil (hidrofóbicos) à superfície. A adesão de plaquetas também foi elevada no ouro. As SAMs hidrofóbicas de $C15CH_3$ induziram a adesão e a activação plaquetária visto as plaquetas terem aderido na sua maioria sob a forma espalhada e dendrítica, o que foi observado por SEM.

Foi desenvolvido um material compósito baseado numa matriz de hidrogel, PHEMA, reforçado com fibras de PET modificadas por ozonação, para aplicação biomédica como um substituto de disco intervertebral. Os resultados mostraram uma dramática diminuição do ângulo de contacto, de 74º, no PET não modificado, para 38°, após 6h de tratamento por ozono em condições específicas. O efeito da hidrofilicidade do PET na adesão ao PHEMA foi seguidamente caracterizado através de ensaios de tracção, e por análise da morfologia das superfícies fracturadas por SEM. A adesão entre o PET e o

PHEMA foi melhorada, como os testes de tracção mostraram. As fotomicrografias obtidas por SEM confirmaram que a melhor adesão entre as fibras de PET tratadas e o PHEMA foi obtida quando as fibras de PET foram tratadas por ozono durante 6 h e imediatamente imersas numa solução reactiva de PHEMA.

Contents

Acknowledgements ..... **iii**

Publications ..... **v**

Abstract ..... **vi**

Resumo ..... **viii**

Contents ..... **xi**

1. Introduction **1**

1.1. Relevance and motivation 1

1.2. Objectives and outlines 3

1.3. State of the art 4

1.3.1. Surface interactions 5

1.3.1.1. Hydrophilicity 6

1.3.1.2. Protein adsorption 7

1.3.1.3. Cell adhesion 13

1.3.2. Self-assembled monolayers as a tool to evaluate surface modifications 16

1.3.3. Implications of surface modification in biomaterials applications 16

1.3.3.1. Intervertebral disc substitutes 16

1.3.3.2. Blood contact devices 19

2. Materials and methods **22**

2.1. Materials and surface modification for intervertebral disc substitutes 22

2.1.1. poly(ethylene terephthalate) (PET) samples preparation 22

2.1.2. Surface modification of PET to enhance its hydrophilicity 22

2.1.2.1. Ultra-Violet radiation 22

2.1.2.2. Graft polymerization of HEMA onto PET 23

2.1.2.3. Surface physical interpenetrating networks (SPIN) of PET and poly(ethylene oxide) (PEO) 23
2.1.2.4. Ozonation 24
2.1.3. Preparation of polyhydroxyethyl methacrylate (pHEMA) hydrogels 25
2.1.4. Preparation of pHEMA hydrogels reinforced with PET fibers 25
2.1.5. Samples characterization 26
2.2. Protein adsorption and platelet adhesion onto SAMs 29
2.2.1. Preparation of SAMs 30
2.2.1.1. Gold substrates 30
2.2.1.2. Monolayer formation 30
2.2.1.3. Surface characterization 31
2.2.2. Protein adsorption using radiolabelling technique 33
2.2.2.1. Fibrinogen (HFG) and Albumin (HSA) solutions 33
2.2.2.2. HFG labelling with Iodine-125 33
2.2.2.3. Quantification of adsorbed HFG to SAMs 34
2.2.2.4. Competitive adsorption between HFG and HSA to SAMs 34
2.2.2.5. Exchangeability of adsorbed HFG with other proteins in solution 35
2.2.3. Platelet adhesion and activation 35
2.2.3.1. Preparation of platelet rich plasma (PRP) 35
2.2.3.2. Quantification of adhered platelets to SAMs 36
3. Results and discussion 39
3.1. Intervertebral disc substitutes 39
3.1.1. Attenuated Total Reflection-Fourier Transform Infra-Red spectroscopy ATR-FTIR 39
3.1.2. X-ray photoelectron spectroscopy (XPS) 40

3.1.3. Contact angle measurements of PET film 42
3.1.4. Scanning electron microscopy (SEM) of PHEMA/ozone modified PET single fiber samples 45
3.1.5. Mechanical characterization 47
3.1.5.1. Tensile strength of PET monofilaments 47
3.1.5.2. Tensile strength tests with PHEMA hydrogels reinforced with ozone-treated PET monofilaments 49
3.1.5.3. Tensile strength tests with PHEMA hydrogels reinforced with ozone-treated PET bundles 50
3.2. Blood contact devices 52
3.2.1. Surface characterisation of gold 53
3.2.2. Surface characterisation of SAMs 54
3.2.3. Protein adsorption 59
3.2.3.1. Quantification of HFG adsorption on different SAMs 59
3.2.3.2. Exchangeability of adsorption 60
3.2.3.3. Competitive adsorption of HFG and HSA to SAMs 61
3.2.3.4. Platelet adhesion and activation to SAMs and gold substrate 63
4. Conclusions and perspectives 70
5. References 72

1. Introduction

1.1. Relevance and motivation

Surface modification is relevant in biomaterials applications as a tool to alter the chemical and physical properties of the surface maintaining its appropriate mechanical behavior. In this context, surface modification can be used to improve the interactions between two different materials and also the biocompatibility of a material with the surrounding tissue.

a) Blood contact biomaterials

Knowledge of the interaction of proteins with surfaces is vital when developing new biomaterials. When any foreign material is introduced into the body proteins immediately adsorb and will determine how the body reacts to the implant. When in direct contact with blood, and if platelets and proteins related with the blood coagulation system are activated, biomaterials are prone to induce the formation of clots.

Gaining an understanding of the type, the amount and the way of blood protein adsorption is essential for the characterization of the biointerfacial processes and also in designing new biomaterials for biomedical applications, such as medical devices and disposable clinical apparatus (vascular prostheses, blood pumps, heart valves) for contact with blood.

Surfaces that adsorb albumin are more hemocompatible since the adsorption of this protein avoids platelet activation and the adsorption of other proteins that could induce the activation of the coagulation system. On the contrary, the adsorption of fibrinogen induces the adhesion and activation of platelets. Therefore, it is important to understand how blood proteins like albumin and fibrinogen interact with biomaterials surface. In a previous research work developed in our laboratory, the effect of surface wettability in protein adsorption was

investigated using self-assembled monolayers (SAMs) prepared with different percentages of a hydrophobic and a hydrophilic functional groups (-CH_3 and -OH, respectively).[1] Results suggested that for a certain percentage of hydroxyl groups on the monolayer surface (65% ± 6 of -OH) some selectivity to albumin adsorption was achieved. The higher degree of albumin exchangeability observed for this surface also suggests that the native albumin conformation was maintained. In the present work, these types of SAMs were prepared and their effect on fibrinogen adsorption and platelet adhesion and activation was studied.

b) Intervertebral disc substitutes

Intervertebral disc degeneration, caused by prolapsed discs, trauma and mechanical related causes, is one of the major causes of low back pain. The most common surgical treatment is removal of the disc (discectomy) and spinal fusion. Another solution is the replacement of the degenerated disc for an artificial disc substitute. The last procedure is gaining popularity since it maintains physiological characteristics of the spine.

The spine consists of a series of roughly cylindrical bones (vertebrae) joined by flexible intervertebral discs. Each disc consists of a soft centre (the nucleus) that is enclosed by a fibrous outer layer (the annulus). The nucleus has a high fluid content and exerts a swelling pressure that is balanced by tension in the annulus. In a damaged disc, the nucleus may cause the annulus to bulge out and, in extreme cases, can even escape through tears in the annulus.

In the development of a total disc substitutes (nucleus, annulus and end-plates) several aspects need to be addressed: preparation of composite intervertebral disc, interface improvement of fiber/matrix and design and preparation of composite end-plates. In the present study it will focus on the interface improvement of fiber/matrix (annulus).

1.2. Objectives and outlines

In general, the most common polymers used in the medical field are hydrophobic. For this reason, the incorporation of functional groups onto polymer surfaces to improve their hydrophilicity, without changing the mechanical behavior of the material, is widely studied. Chemical modifications of biomaterials surfaces are normally used to increase the biocompatibility and the adhesion between different biomaterials.

The aim of this work was the modification of polyethyleneterephtalate (PET) surfaces in order to enhance their interaction with the hydrophilic matrix (polyhydroxylethylmethacrylate, PHEMA) and to produce a strong bond between these two polymers.
The effect of wettability on the adsorption of the plasma protein human fibrinogen (HFG), and on the platelet adhesion was also studied using model surfaces. Self-assembled monolayers (SAMs) containing mixtures of longer chain methyl- and shorter chain hydroxyl-terminated alkanethiols on gold were used to produce a range of surfaces with different wettabilities and exposed functional groups.

This thesis is organized as follows. In Chapter 1, “Introduction”, the state of the art regarding surface interactions, self-assembled monolayers and implications of surface modification in biomaterials applications is presented. Chapter 2, “Materials and methods”, deals with materials and surface modification for intervertebral disc substitutes and protein adsorption and platelet adhesion onto SAMs. In Chapter 3, “Results and discussion”, the methodologies developed in the previous chapter are applied to intervertebral disc substitutes and blood contact devices. Finally, in Chapter 4 conclusions and suggestions for future work are presented.

1.3. State of the art

A biomaterial is defined as a material intended to interface with biological systems to evaluate, treat, augment or replace any tissue, organ or function of the body.[2] The study of biomaterials involves investigations into their relevant characteristics, i.e., their mechanical, thermal, electrical and especially their surface properties, for the surface is in contact with living tissues. Thus, the study of these surfaces is crucial to determine their biological behaviour and to evaluate their hydrophobic or hydrophilic character.[3]

Biomaterials are used to manufacture prostheses, implants, and surgical instruments. Designed not to provoke rejection by our bodies (skin, blood, bone, etc.) they can be natural (collagen, cellulose, etc.) or synthetic (metallic, ceramic, plastic, and others). Dental crowns and contact lenses use biomaterials. Employed in plastic and reconstructive surgery, used to make the tools needed to examine the human body, and expected to improve the deficiency of an organ, biomaterials must be biologically compatible with the organism.

The first generation comprised mostly metals, alloys and polyester materials. Later, a second generation emerged, labeled “medical grade”, which makes use of non-toxic materials easily accepted by patients. Although these foreign objects are well tolerated, they cannot completely integrate with living tissues. The third generation now under research focuses on hybrid materials that associate inert and living material created by tissue engineering (for example, skin cell cultures). Many biomaterials have been used due to their bioinertness or bioactivity,[4-10] depending on the specific aim, but also on availability.

At present, research on biomaterials science is combining biomaterials, biotechnology and molecular biology, in order to have biomaterials with a specific biological functionality.[11-39]

1.3.1. Surface interactions

Biocompatibility has been defined as the ability of a material to perform with an appropriate host response in a specific application. [40]

As it is requested, biomaterials are intended to biologically function properly; this specificity leads to the incorporation of biologically active species at a molecular level. The study of the interactions of biologically active species with materials is possible through the preparation of structures consisting on materials, cells and proteins, that promote a specific biological response after implantation.[3-7, 11-39, 41, 42]

The interaction of those species with the surface of biomaterials is usually responsible for the biological behavior of implanted materials. The control of the protein monolayer adsorbed at the moment of implantation is an important parameter.

Blood-material interactions trigger a complex series of events including protein adsorption, platelet and leukocyte activation/adhesion, and the activation of complement and coagulation: there processes are highly interlinked (Fig.1)

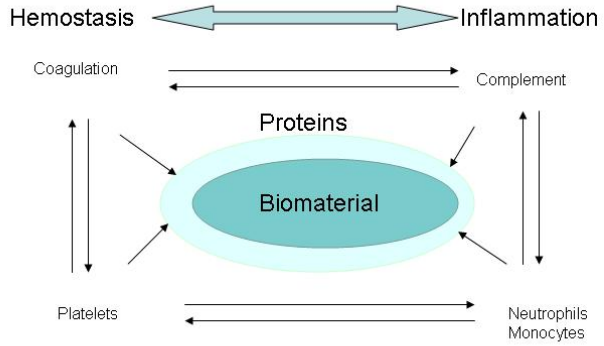

Figure 1. Overview of blood-material interactions showing the components relevant to thrombosis. Adapted from Gorbet and Sefton.[43]

Several surface properties considerably influence the whole cascade of events that will dictate

the biological performance of a biomaterial. Among these properties, hydrophilicity plays a key role since it is a controlling factor of protein adsorption and cell adhesion.

1.3.1.1.Hydrophilicity

Hydrophilicity is the affinity for water of a substance caused by isolated charges or by highly polar groups able to interact strongly with the polar water molecules.

In general, the major polymers used in industry are hydrophobic, thus are not very useful for many biotechnological process.[44] For this reason, the incorporation of functional groups in the polymer surfaces to improve the hydrophilicity, without changing the mechanical behavior of the material, has been widely studied.

Hydrophobic surfaces are distinguished from hydrophilic by virtue of having Lewis acid or base functional groups available for water interactions.[45]

Hydrophobic interactions play an important role in protein adsorption. In case of a hydrophobic surface, proteins adsorb on the surface via hydrophobic interactions.

In these types of interactions, compact monolayers are formed, there is no desorption and only a slow partial exchange between adsorbed and dissolved protein occurs. Proteins are predisposed to minimise exposition of their hydrophobic groups to the aqueous environment. The adsorption process is often entropically driven with the gain in entropy arising from dehydration of the adsorbent surface and structural rearrangements inside the protein molecule.[46-49]

1.3.1.2. Protein adsorption

There are biological responses to implanted biomaterials, including the clotting of blood and the foreign body reaction. The basis for these reactions is the adsorption of adhesion proteins to the surface of the biomaterials that are recognized by the integrin receptors presented in most cells. In seconds to minutes, a monolayer of proteins adsorbs to almost every surface.[50] Fibrinogen and albumin are the major constituents of adsorbed proteins. Other proteins are adsorbed in smaller amounts like von Willebrand factor (vWF), fibronectin, α- and β-globulins, the coagulation factors XI and XII and HMWK (high-molecular-weight kininogen).

Proteins are complex molecules comprised of amino acid copolymer (polyamide) chains that interact with each other to give the molecule a three-dimensional structure.[51] Protein functional properties depend on their three-dimensional structures. Protein structure has been described at four different scales (Figure 2).[52, 53] The primary structure refers to the order and number of amino acids in a copolymer chain. From the 20 amino acids building blocks (residues), 8 have nonpolar side chains, 7 have neutral polar side chains and 5 have charged polar side chains. Secondary structure results from hydrogen bonding associated with the amide linkages in the backbone of the proteins to form structures as α-helix and β-pleated sheet. Tertiary structure results from intramolecular associations, including ionic interactions, salt bridges, hydrophobic and hydrophilic interactions, hydrogen bonding and covalent disulphide bonds. Quaternary structure results from associations between amino acid chains.

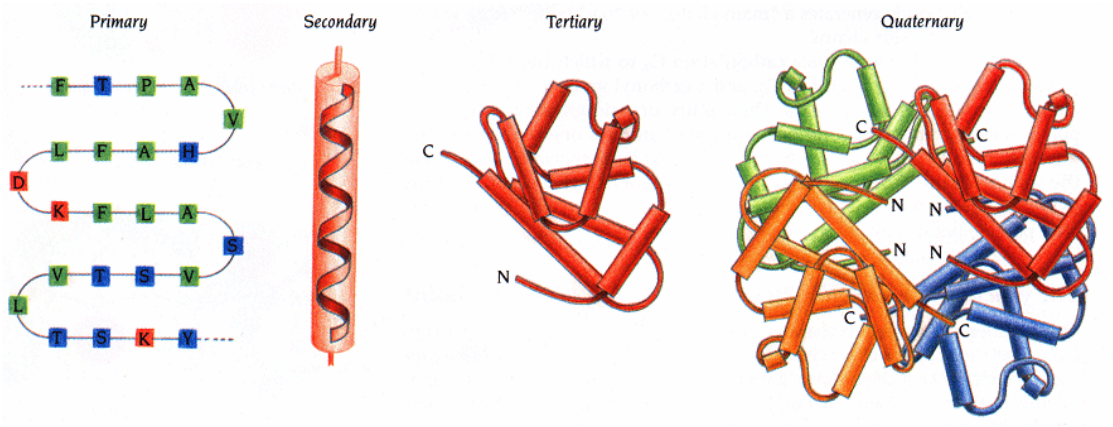

Figure 2 . Schematic representation illustrating the four structures of the proteins.[53]

Proteins are large and have a very folded structure corresponding to a large number of different aminoacids. Thus, proteins have different surface domains with hydrophobic, hydrophilic and negatively or positively charged character.[46,52,54] The charges, positive and negative, are distributed around the exterior of the protein, depending on the pH and the ionic strength of the media. As a consequence, they are highly surface active.[47] Figure 3 schematically shows the interactions of a protein with a surface with comparable character.[46]

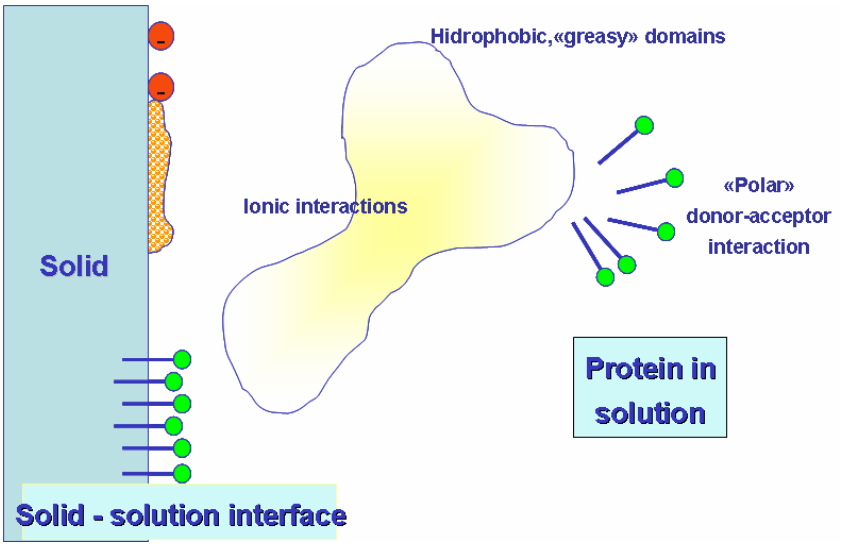

Figure 3. Schematic view of protein interacting with a well characterised surface. Adapted from Andrade and Hlady.[46]

Several factors contribute for the complexity of the protein adsorption process, such as properties of the proteins, of the solid surface, and environmental conditions.[55]

Many authors have been studying protein adsorption, but a lot of aspects related with mechanisms of protein adsorption are still unclear.[46-48, 55-57] Hydrophobic and electrostatic interactions and the structural stability of the protein are the most important events involved in protein adsorption process. [46-49, 58-60]

Plasma Proteins

Adsorbed proteins affect biocompatibility in ways that are not completely understood. Fibrinogen has been extensively studied because platelets involved in thrombosis and hemostasis have a receptor for this protein. Adsorbed fibrinogen is often proposed to decrease biological tolerance. Evidence suggests that fibrinogen adsorbed from blood to substrates upon which the protein readily denatures may in fact promote biological behaviour.[39]

Fibrinogen

Fibrinogen is an exceptionally elongated molecule (Figure 4) made up of three globular units connected by two rods (Figure 5) with a molecular weight of 340,000 dalton.[61]

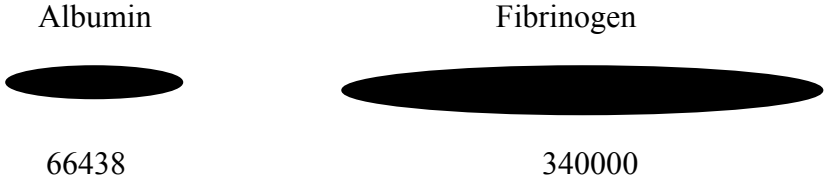

Figure 4. Molecular weights and shapes of albumin and fibrinogen. [62]

Fibrinogen is produced in the liver and has a plasma concentration between 2 to 4 mg/mL.[63] It contains 10% charged residues and it is negatively charged at pH 7.4. The isoelectric point (IEP) of fibrinogen is 5.5 and its dimensions are 5 x 5 x 47 nm^3.[64]

Fibrinogen is important to the activation and aggregation of platelets.

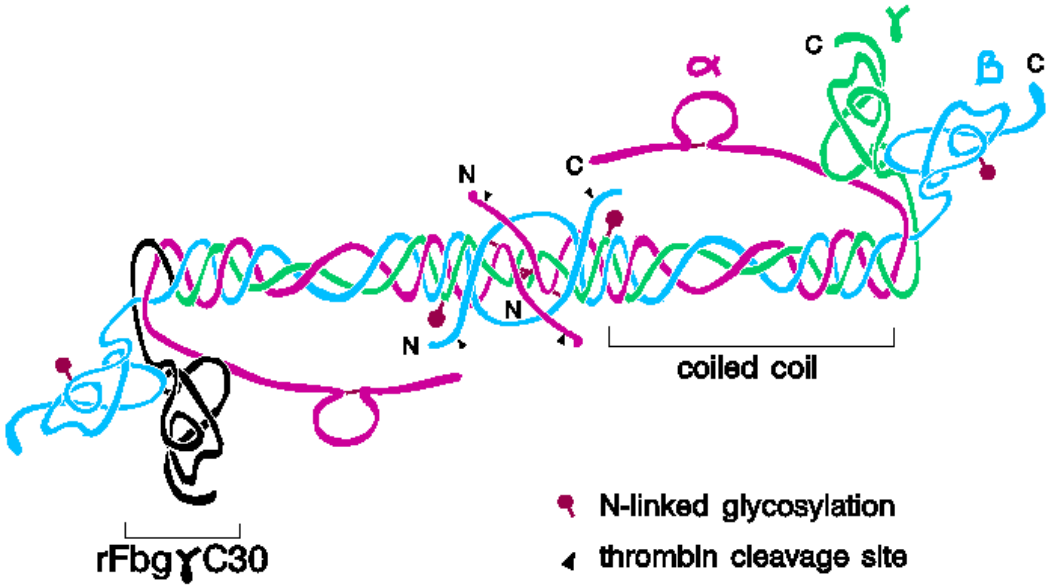

Figure 5. Schematic representation of human fibrinogen. [65]

Albumin

Albumin is the most abundant protein found in blood. Albumin is almost 60% of the total protein in blood serum in a concentration of ~ 40 mg/mL (human adults). It is an ellipsoid molecule (Figure 4) and consists of a single polypeptide chain containing 585 amino acids with 17 intrachain disulphide bounds.[66, 67] Albumin is one of the plasma proteins that is not a glycoprotein, and it has the lowest molecular weight of plasma proteins with a molecular weight of 66,438 dalton.[66]

Albumin contains a large number of polar and charged residues, with an isoelectric point of 4.7, indicating that in physiological conditions this protein has a negatively charge.[66] The protein was described to have an ellipsoid form with dimensions of 3.8 x 3.8 x 15 nm^3.[68] Albumin is mainly adsorbed on a hydrophobic surface and least adsorbed on a negative charged surface.[62]

Albumin is very important in the field of biomaterials due to its "nonthrombogenic" effect.

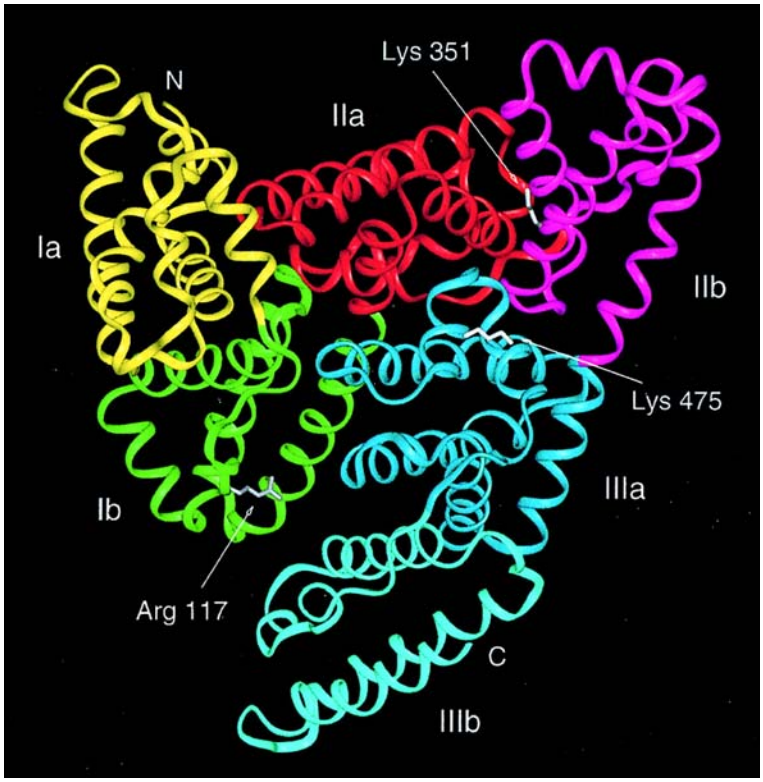

Figure 6. Schematic drawing of the HSA molecule. Each subdomain is marked with a different color (yellow for subdomain Ia; green, Ib; red, IIa; magenta, IIb; blue, IIIa; and cyan, IIIb). N- and C-termini are marked as N and C, respectively. Arg117, Lys351 and Lys475, which may be binding sites for long-chain fatty acids, are colored white.[69]

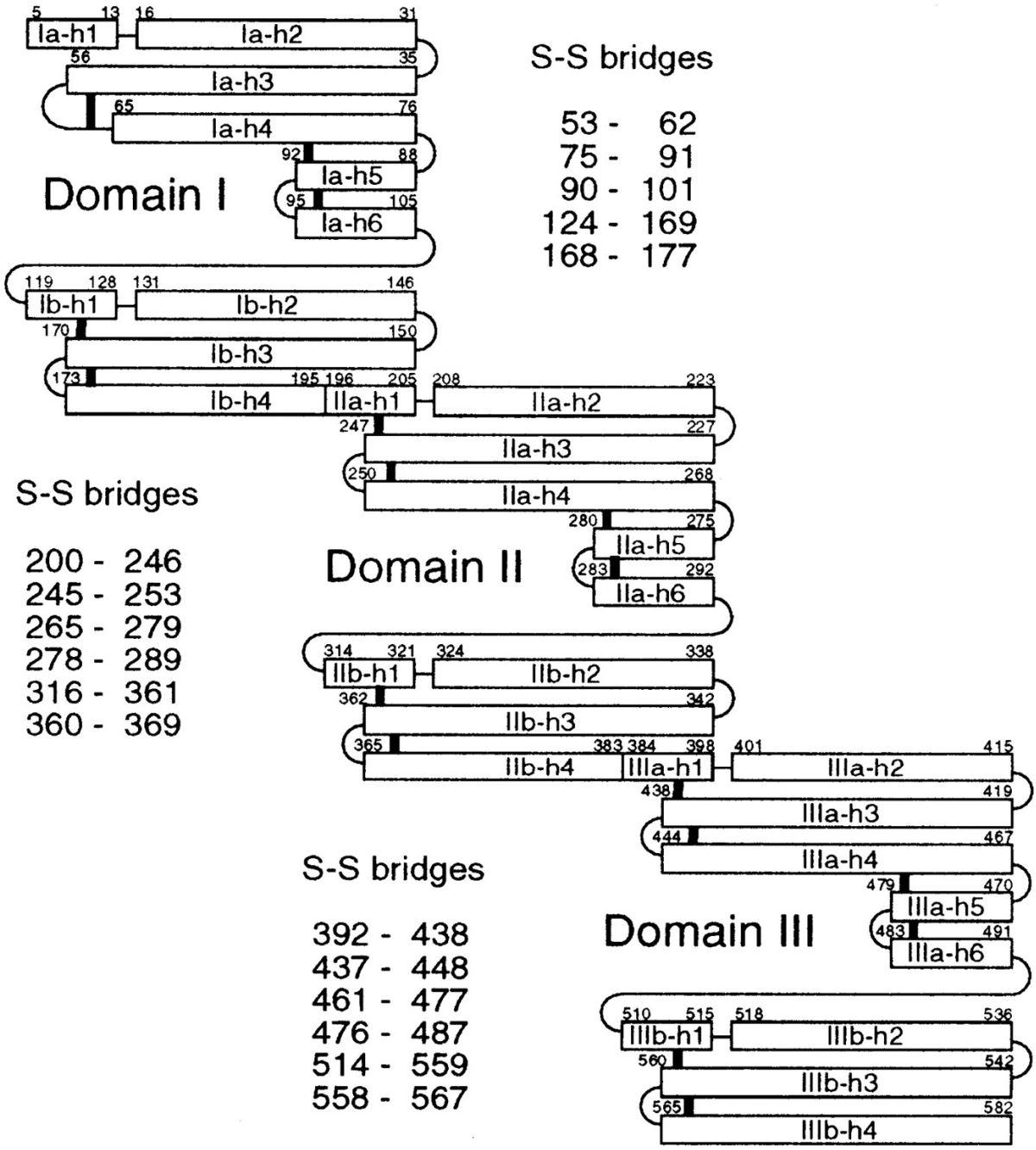

Figure 7. Schematic drawing of secondary structure elements and disulfide bridges of HSA. Helices are represented by rectangles, and loops and turns by thin lines. Disulfide bridges are drawn with thick lines. The sequence nomenclature is derived from Minghetti *et al*. (1986).[70]

1.3.1.3. Cell adhesion

Platelets (thrombocytes) are non-nucleated, disk-shaped having a diameter of 3-4μm and an average volume of 10 x 10^9 mm^3. Platelets are produced in bone marrow, circulate at an average concentration of about 250.000 cells per microliter of whole blood, and occupy approximately 0.3% of the total blood. Platelets functions are designed to arrest bleeding from injured blood vessels through formation of a platelet plug, and stabilize the initial platelet plugs by catalyzing the coagulation reaction leading to the formation of fibrin.[71] In nonstimulated state, the platelet discoid shape is maintained by a circunferencial bag (cytoskeleton) of microtubes (Figure 8).

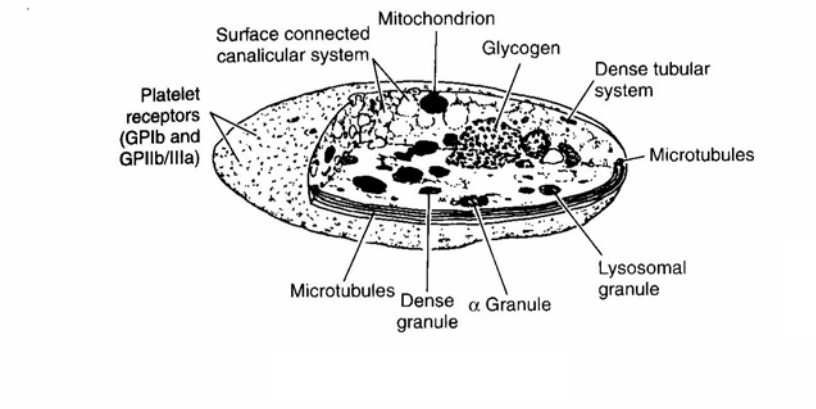

Figure 8. Platelet structure.[71]

The external surface coat of the platelet contains membrane-bound receptors (e.g., glycoproteins Ib and IIb/IIIa) that mediate the contact reactions of adhesion and aggregation. Platelets contain substantial quantities of muscle protein (e.g., actin, myosin) that allow the internal contraction when platelets are activated. The secretion of their products such as adenosine diphosphate (ADP) stimulates other platelets, which leads to a platelet aggregation and the formation of a thrombus (Figure 9). Following protein adsorption to surfaces, platelets

adhere and release α-granule contents, such as platelet factor 4 (PF4) and β-thromboglubin (β-TG), and dense granule contents, such as ADP. Trombin is generated locally through coagulation reactions.

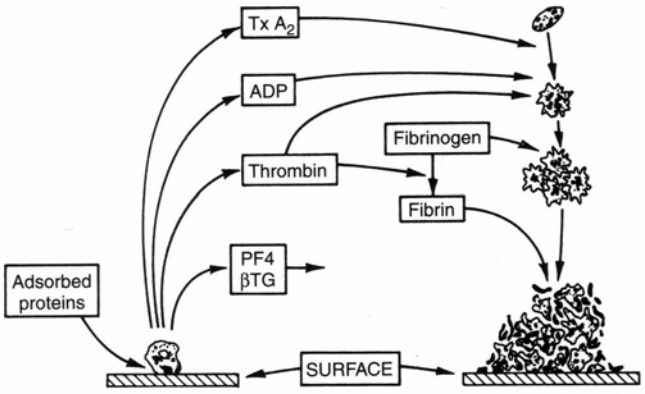

Figure 9. Platelet reactions to artificial surfaces.[71]

Platelets have been extensively studied due to their role in thrombogenesis. Platelet activation can bring out a variety of physiologic cellular responses including shape change, biochemical membrane alterations, induction of membrane procoagulant activity, release of granule contents, initiation of aggregation and the release of procoagulant microparticles or small membrane vesicles from the surface. The release of α-granule contents leads to P-selectin expression on platelet membranes and platelet aggregation is mediated by fibrinogen binding to GPIIb/IIIa receptors.[72-74] Thrombin binds directly to platelet thrombin receptors and is responsible for the platelet aggregate formation by activating platelets, which produce more thrombin, stimulating ADP release, and stimulating the formation of fibrin, which stabilizes the platelet thrombus. Thrombin is responsible for catalysing the conversion of fibrinogen to fibrin in the final step of the coagulation cascade (intrinsic or extrinsic pathway). The generation of thrombin results from the activation of contact phases in intrinsic pathway of coagulation or from more indirect mechanism involving platelets or leukocytes and extrinsic pathway (Figure 10).

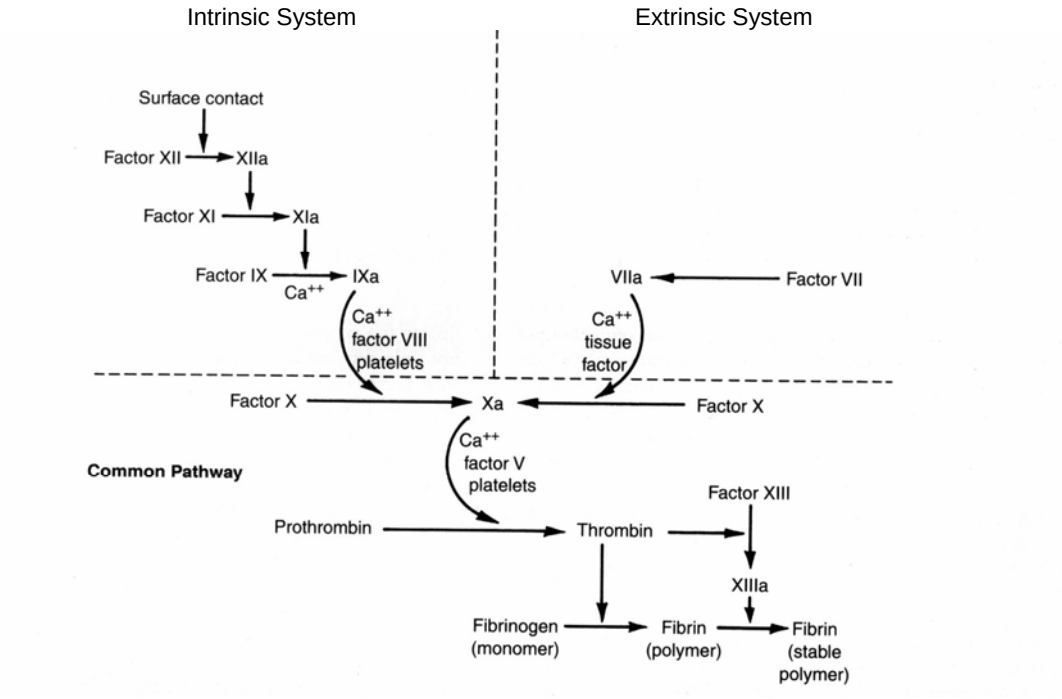

Figure 10. Mechanism of clotting factor interactions.[71] Clotting is initiated by either an intrinsic or extrinsic pathway with subsequent factor interactions that coverage upon a final, common path.

The extent of platelet spreading can be examined by categorizing platelet shapes into five morphological forms describing increasing activation.[75] These are discoid or round (R), dendritic (D), spread dendritic (SD), spreading (S), and fully spread (FS). The spreading stages are shown in Figure 11 and defined in the legend.

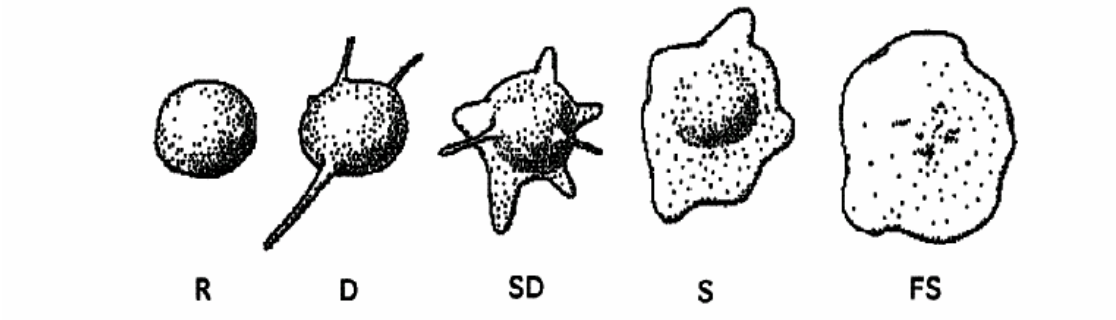

Figure 11. Diagrammatic representation of platelet spreading divided into five shape categories for analyses. These stages are defined as follows[75]: round (R): no pseudopodia present; dendritic (D): one or more pseudopodia with no evident flattening; spread dendritic (SD): one or more pseudopodia flattened, hyaloplasm not spread between pseudopodia; spreading (S): hyaloplasm spread between pseudopodia; and fully spread (FS): hyaloplasm extensively spread, no distinct pseudopodia.

1.3.2. Self-assembled monolayers as a tool to evaluate surface modifications

Different approaches to functionalization of biomaterials exist. The self-assembled monolayer (SAM) technique has been successfully applied on chemically inert materials like polymers to graft various functional groups to the surface. This technique can provide a well-defined, highly oriented surface when the carbon chain length of the alkanethiols is longer than 10 carbon atoms.[76] Furthermore, a wide range of chemical groups both in the alkyl chain and at the chain ends can be used, which has allowed surfaces with specific interactions to be produced with fine chemical control trough the SAM technique. [77, 78]

Many researchers have employed this technique to study interactions between the biological environment and synthetic biomaterials and to improve the materials biological interaction.[79-84] Surface functionalization may provide a way to transform a bio-inert material into a biomimetic or even bio-active material by coupling of protein layers to the surface. Tengvall et al. studied the effect of methyl- and hydroxyl-terminated alkanethiols on tissue compatibility *in vivo* and *in vitro*.[85] They noted that fibrinogen tended to adsorb onto pure gold and methylated surfaces while the cells were less attached to the methylated SAM.

1.3.3. Implications of surface modification in biomaterials applications

As previously outlined, the surface properties of a biomaterial are fundamental for its biological performance since it is the surface that will contact the biological environment. However, in many applications biomaterials with a set of properties are required, such as mechanical, but their surface may not match the required needs. As a consequence, surface modifications can be carried out to tailor the biomaterial surface to the desired biological behavior. Alternatively, surface modifications can be performed to improve the interactions

between biomaterials designed for a complex biomedical device.

1.3.3.1. Intervertebral disc substitutes

An intervertebral disc is constituted of two components: the nucleus pulposus and the annulus fibrous. Both are anchored to the vertebral bodies by the end-plates (Figure 12). The intervertebral disc is a fibrocartiloginous complex that forms the articulation between the bodies and the vertebrae. The essential function of the nucleus is to resist and distribute compressive forces within the spine and the most important function of the annulus is to hold out tension.

Figure 12. View of an intervertebral disc

The intervertebral disc consists principally of collagen fibbers embedded in a proteoglycan-water gel. The latter component develops a large swelling pressure which enables the disc to resist compressive properties. Water is the main constituent of the disc, occupying 65 to 85 per cent of the tissue volume depending on age and region. The structure of the intervertebral disc, as well as its biomechanical and transport properties, are unique and very complex.

Designing an appropriate intervertebral disc substitute represents the challenge of biomaterials scientists involved in the European project: Novel intervertebral Disc Prostheses (nº G5RD-CT-2000-00267). Part of this thesis has been carried out according to the project work-plan, which is to modify the surface of PET films in order to achieve a homogeneous and cohesive PET/PHEMA composite consisting on a hydrophilic matrix and hydrophobic polymer fibers for annulus application.

Hydrogels are polymeric networks held together by covalent bonds and other cohesive forces such as hydrogen or ionic bonds. Attributes such as permeability to small molecules (i.e. metabolites) and their soft consistency are important properties that make them very attractive as matrix for composite soft tissue prostheses. Composites made of poly (2-hydroxyethyl methacrylate), PHEMA reinforced with PET fibers have been used to design ligament, tendon and intervertebral disc prostheses.[86-88] Their long-term mechanical performance in swollen state is limited by the poor interface properties between the fiber and the matrix.

Many technologies concerning polymer surface modification are available, such as ozonation, plasma treatment, grafting of PEO onto PET surfaces. Ozonation consists on the surface exposure to the ozone beam as an easy way to create hydrophilic groups.[89-92] This exposure results in an increase in the surface energy of the polymer trough the breaking of molecular bonds on the surface and the addition of polar groups. It has been used in the surface characterisation of fiber-supported hydrogels.[89] Fiber-supported hydrogels were prepared by ozone-induced grafting onto polypropylene fibers; ozonation was investigated by studying the hydroperoxide concentration as a function of chain scission. Ozone-induced grafting was used for the preparation of various hydrogels supported onto fibers. Grafted hydrogels were prepared by changing the composition of the monomer mixture used for graft polymerization.

Another technique for surface modification of PET is plasma-treatment by NH_3 /H_2 radio frequency glow discharges (RFGD).[93] The plasma-treatment aimed to graft NH_2 groups onto

the surface of PET. The combined use of plasma and surface analyses allowed clarification of the chemical mechanisms involved in the surface processes and to understand the effect of the experimental parameters on the extent of the surface modification.

Another study refers to surface physical interpenetrating networks of poly (ethylene terephthalate) and poly (ethylene oxide) with biomedical applications.[94] PET films were modified by diffusing PEO into the surface of PET, which was swollen in a mutual solvent. Subsequent rapid deswelling in a nonsolvent for PET resulted in the stable entrapment of the PEO within the surface of PET. The PET/PEO systems produced by this technique were phase-mixed nonequilibrium surface structures, kinetically stable below the Tg for PET. This surface structure is referred as a surface physical interpenetrating network (SPIN).

Another surface modification is achieved by grafting polyethylene oxide (PEO) onto polyethylene terephthalate surfaces.[95] Several approaches have been used to modify polymer surfaces with PEO. Among them are those techniques that involve covalent grafting of PEO into a base polymer such as PET, polymerization of a monomer having a pendant PEO chain, incorporation of PEO into a base polymer by block copolymerization, or direct adsorption of PEO-containing surfactants.

1.3.3.2. Blood contact devices

Synthetic biomaterials have been evaluated and used for a wide range of medical applications. The ultimate aim in medicine, besides prevention, is the healing of diseases and repairing damage after injuries. The task of engineers, material scientists and physicists is to provide an optimal system for these applications. Polymers can be used either as bioinert or bioactive materials, depending on the application. Hydrophobic silicone is a widely used material due to its good biocompatibility and mechanical properties. The medical devices that find either

intra- or extracorporeal application hold a wide spectrum of synthetic materials: polyethylene, polypropylene, polyvinylchloride (PVC), polyester, polystyrene, polyurethane, silicone, polysulphone, polyamide, polytetrafuoroethylene, their derivatives, etc. Although these products have excellent physical properties, they were nonetheless developed primarily for industrial use and only later found their way into biomedicine. Thus, all these synthetic materials display more or less the same disadvantage: an incompatibility with blood and tissues. Through contact with blood, this incompatibility can provoke a pathophysiological response from the organism, similar to that of traumatic shock. This extensive contact causes a massive activation of the cellular defense systems against the supposed `invader', and with that the human body boosts the various cascade reactions into motion. Heparin-coating was recognized as an improvement on hemocompatibility of the materials used in biomedical applications. The attempt to coat the artificial surfaces with heparin, an anticoagulant that imitates the antithrombogenic effects of heparansulfate at the endothelium, illustrates the first step towards attaining better hemocompatibility.[96]

A popular method to improve the blood compatibility of biomaterials is to increase surface hydrophilicity by incorporating a hydrogel at the surface. Hydrogels permit the retention of large amounts of water without dissolution of the polymer itself, which makes them very similar to physiological tissues. A variety of surface-grafted copolymers were prepared and evaluated for platelet consumption in a baboon shunt model of arterial thrombogenisis by Hanson et al.[97] Few platelets were found adherent to the graft surface.

Immobilization of poly(ethylene glycol) (PEG) is a very popular means of making a biomaterial surface more protein and cell resistant.[95] It is clear that incorporation of PEG reduces the cell adhesion (including platelets) and protein adsorption when compared with hydrophobic surfaces.

Albumin coating is another technique used to decrease thrombogenicity. The early

observation that surfaces coated with albumin did not support protein adsorption and platelet adhesion,[46] led some investigators to lower material thrombogenicity by either albumin coating or enhancing the affinity of albumin for surfaces via alkylation. It is widely recognized that albumin adsorption lowers material thrombogenicity, since it does not possess the peptide sequences to enable interaction with cells (platelets and leukocytes) or the enzyme receptors in the coagulation cascade.

Self-assembled monolayers have been a useful template to nucleate or organize ordered, designed biomaterials.[98] The advantages of self-assembly films are their high order and orientation and well-defined head-group geometry that exposes only one functional group to the outside. With this technique it is possible to obtain a surface with desired functionalities and control protein adsorption.

2. Materials and methods

2.1. Materials and surface modification for intervertebral disc substitutes

In order to increase PET hydrophilicity, several surface modifications methods were used to find out the one that would provide the best results.

PET bundles (Dacron Type DRT: 9-0329) with an average diameter of 0.75 mm were provided by Institute of Composite and Biomedical Materials (ITC), Naples, Italy. Reagents were used without any further purification.

2.1.1. PET samples preparation

PET sheets were cut into 60×30 mm^2 for all treatments performed. Before any modification, samples were consecutively washed with ethanol, water (distilled and deionized) and ethanol, for periods of 3 min, in an ultrasonic bath. After being thoroughly washed, samples were dried overnight in a vacuum oven RAYPA EV-50 at 30 °C, and stored in a dessicator over silica before further use. The same procedure was used with fibres.

2.1.2. Surface modification of PET to enhance its hydrophilicity

2.1.2.1. Ultra-Violet radiation

The effect of a physical treatment (UV radiation) was carried out at ISEP-Instituto Superior

de Engenharia do Porto on PET films using different times (10, 20, 30, 50, 100, 200, 400, 600 and 800 hours) with 83ºC as temperature, 254nm of wavelength and 20 W.

2.1.2.2. Graft polymerization of HEMA onto PET

The graft polymerization of poly (hydroxylmetacrylate) (PHEMA) onto PET was carried out using ceric salt as an initiator.[99]

2-hydroxyethyl methacrylate (HEMA, Aldrich, Mw 130.14) was distilled at 110ºC, under reduced pressure. PET films were immersed in the monomer aqueous solution (13.3% v/v) for 15 minutes, under constant stirring and a nitrogen stream. The ammonium cerium (IV) nitrate ($(NH_4)_2Ce(NO_3)_6$, Merck) (2.2 g) was diluted in nitric acid solution (HNO_3, Merck) (5 mL). This solution was then diluted in water (15.3% v/v), added to the previous solution, and the reaction was allowed to proceed at room temperature, for 180 min. Finally, PET films were extracted 4 times with 250 mL deionized water at 70ºC for 24h with agitation of 250 rpm. Samples were then dried in a vacuum oven at 60ºC overnight. Polyurethane was used as a control.

2.1.2.3. Surface physical interpenetrating networks (SPIN) of PET and poly (ethylene oxide) (PEO)

This treatment consists of diffusing PEO into the surface of PET, which is swollen in a mutual solvent. Subsequent rapid de-swelling in a non-solvent for PET results in the stable entrapment of the PEO within the PET surface. [87]

Trifluoroacetic acid (TFAA, Merck) was used as the mutual solvent. TFAA was diluted by 20% (v/v), by adding an aqueous PEO (Aldrich, Mw 10 000) solution (0.4 g/mL). PET fibres

were immersed in this solution for 60 minutes, using room temperature and 50ºC, with and without stirring, in order to swell, thus allowing diffusion of PEO at the surface. The swollen PET was then collapsed by addition of excess water, thus entrapping PEO chains at the surface.

2.1.2.4. Ozonation

Ozone treatments were carried out at RAÍZ - *Instituto da Investigação da Floresta e Papel* (Aveiro, Portugal). This process exposes the polymer surface to ozone, in order to increase the number of oxygen functional groups.

PET films (10 × 20 cm^2) and monofilaments mounted into a stainless steel support, were treated with ozone (O_3) gas in a sealed cylindrical (36 × 35.8 cm^2) stainless steel reactor (Scheme 1). The ozone was generated by a Fischer Ozone 502 apparatus that was coupled to an oxygen supplier (medical grade, Gasin, Portugal) at a flow rate of 400 L O_2 per hour. In these conditions, ozone is formed at a concentration approximately of 0.078 mmol O_3 per liter of O_2, as determined by iodometric-thiosulfate titration. Samples were treated for up to 6 hours.

After the ozonation treatment, part of the modified PET fibers were immediately immersed into a HEMA reactive solution in order to avoid further surface modifications. Samples were kept at room temperature for ca. 90 minutes and then stored overnight at 5ºC.

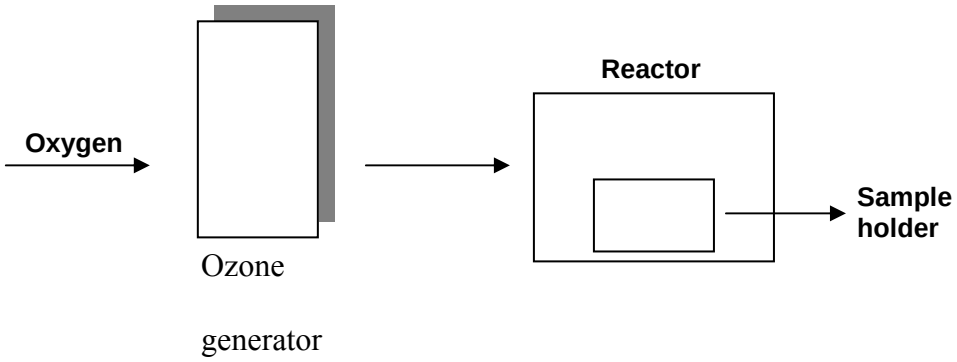

Scheme 1- Schematic diagram of the reactor.

2.1.3. Preparation of PHEMA hydrogels

Typically, PHEMA samples were prepared by adding 0.5 wt-% of ethylene glycol dimethacrylate (EGDMA, Aldrich), as crosslinking agent, 0.1 wt-% of 2,2-azobisiso-butyronitrile (AIBN, Fluka), as initiator, to 2-hydroxyethyl methacrylate (HEMA, Aldrich) monomer.[100] After homogenization, the solution was bubbled with N_2 gas for 20 min. The reactive solution was polymerized into a PTFE (polytetrafluoroethylene) (Teflon®) mould (60x10x1 mm^3) (Figure 13). The polymerization and curing process was performed at 80ºC for 2h30 min in a preheated (80ºC for 1h) oven. After cooling in the oven, each sample was placed in bidistilled water overnight at room temperature to remove any residual monomer.

Figure 13. Teflon mould for samples preparation.

2.1.4. Preparation of PHEMA hydrogels reinforced with PET fibers

In order to study the interface between PET bundles/monofilaments and the PHEMA hydrogel matrix, samples of the two materials were prepared. Test samples were prepared by

pouring the reactive solution in flat polytetrafluoroethylene (PTFE) (Teflon®) moulds. PET bundles/monofilaments were attached to the bottom of the mould with temperature-resistant adhesive tape (3M), prior to pouring the solution. After obtaining the materials as previously described, standard tensile samples (with a cross section of 4x1 mm^2) containing the bundles/monofilaments were cut.

2.1.5. Samples characterization

i. Attenuated Total Reflection - Fourier Transform Infrared spectroscopy (ATR - FTIR)

Modified films were analyzed in a Perkin Elmer 2000 FTIR spectrophotometer, using an ATR accessory (Split Pea). Each sample was run at a spectral resolution of 4 cm^{-1}. 100 scans were acquired.

ii. X-ray photoelectron spectroscopy (XPS)

The surface composition of PET film was determined by XPS in VG Scientific Escalab 200A equipment using magnesium K_α (1253.6 Ev) radiation at 15 kV, 300W, a spot size of a few mm^2, and a take-off angle of 90°. Survey spectra were obtained over a range of 0-1150 eV with analyzer energy of 50 eV. High-resolution spectra of C 1s and O 1s were collected in analyzer energy of 20eV and the atomic concentrations were quantified using tabulated sensitivity factors. Two samples were analyzed: one prepared (as described in 3.1.1.) and one in the as-received state. An XPS peak fitting program (XPSPEAK Version 4.1) was used to fit the spectra. The charging correction was made according to the aromatic carbon using the

binding energy of 284.70 eV.

iii. Contact angle measurements of PET films

In order to evaluate possible ageing of the surface treatments, PET films were analyzed by contact angle measurements 24 hours after ozone treatment and storage at 5ºC.

Wettability studies were performed using an Optical Contact Angle Device OCA15, provided with an electronic syringe unit (both from Dataphysics), and connected to a charge-coupled device (CCD) video camera. The equipment software, SCA20, was used for image analysis and calculation of contact angles. The testing liquid was distilled water, presenting conductivity not greater than 1 μS/cm. The measurements were carried out at 25ºC, inside a thermostatted environmental chamber, previously saturated with a pool of the liquid sample.

The samples used for wettability studies were immediately analyzed after drying. The samples were cut into squares (20×20 mm^2), and nitrogen was used to eliminate eventual dust particles from the surface. Static contact angles were measured by the sessile drop method, drop profiles being fitted to the Young-Laplace equation when contact angle ≥ 70º and fitted to the Elipse equation when the contact angle is between 30º and 70º. Sessile drops of 4 μL of water were deposited on the membrane surface, using a Hamilton syringe fitted with a 0.52 mm needle. Time-dependent measurements were made, and the experimental contact angles extrapolated to time zero. Measurements were taken every two seconds, for a period of 300 s. A minimum of 5 drops was used per sample. Both sides of the film were analyzed.

iv. Mechanical characterization of PET fibres, PHEMA hydrogels and PHEMA/PET fibres samples

The PET monofilaments were inserted into polypropylene (PP) cards (Figure 14) as follows. In a first step, the monofilament was fixed in a groove on one side, with a small piece of adhesive tape (3M®). Afterwards, the fiber was stretched and fixed into the groove at the opposite side, using again the adhesive tape. Cardboard tabs were prepared with two lengths: 30mm and 40mm. The PET single fibres (monofilaments) were mounted on cardboard tabs to provide the appropriate gage length. The mechanical testing was performed at room temperature on an Instron 4204 machine equipped with a 10 N load cell. The tensile deformation was imposed with a mobile clamp moving at a constant speed of 10 mm min^{-1} per ASTM D3379/75. These tests were carried out at Institute of Composite and Biomedical Materials (ICBM), National Research Council and Interdisciplinary Research Centre in Biomaterials, University of Naples 'Federico II', Naples, Italy.

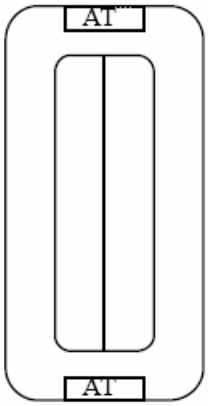

Figure 14. Front view of the polypropylene card with the PET fiber. Dashed line: PET fiber; AT: adhesive tape.

After obtaining rectangular samples of PHEMA containing the fibers, standard samples were cut, in order to perform tensile strength tests and evaluate the adhesion of PET fibres to PHEMA hydrogel.

Tensile strength tests of samples were carried out at INEGI - Instituto de Engenharia Mecânica e Gestão Industrial, Universidade do Porto (Porto, Portugal), using a TIRA test 2705 tensile tester with Tira ZD1 software. The samples were hold at 2 bar and tested at a speed of 100 mm/min using a load-cell of 20 N (monofilaments) or 5 kN (bundles). The testing conditions were 22 ± 1ºC and 50 ± 5% of relative humidity.

v. Scanning electron microscopy (SEM) of PHEMA/ozone treated PET fibres samples

Polymer specimens to be examined by SEM were coated with a thin layer of sputtered gold. An Ion Sputter JEOL JFC 1100 was used to prepare the samples of PET film, fibres and PHEMA hydrogel/PET fibres composite.

The samples were analyzed after drying overnight at 50ºC. After mechanical tests the fracture surfaces of PHEMA/PET samples were observed using a scanning electron microscope JEOL JSM-6301S at 15 kV. The samples were carbon coated.

2.2. Protein adsorption and platelet adhesion onto SAMs

To be aware of the mechanism of protein adsorption and platelet adhesion at the molecular scale requires the use of stable models with a well-defined surface structure. Self-assembled monolayers (SAMs) of alkanethiols on gold are well-ordered organic surfaces with well-controlled surfaces properties. This fact associated with their easy production makes this class of surfaces a very useful model for fundamental mechanistic studies of protein adsorption and platelet adhesion.

2.2.1. Preparation of SAMs

2.2.1.1. Gold substrates

Gold substrates were prepared using an automated, load locked ion beam deposition system (Nordiko N3000). Details on the machine can be found elsewhere.[101] The chromium (5 nm) and gold (25 nm) films were deposited by ion beam sputtering from gold and chromium targets (99.9% purity) onto silicon wafers (polished/etched, crystal orientation <100>, from AUREL Gmbh). The thin layer of chromium was used to improve adhesion of gold to silicon. Deposition rates are 0.050 nm/s for chromium and 0.033 nm/s for gold. Deposition pressure was $3.5x10^{-5}$ Torr. The wafers were diced into pieces (1 x 1 cm^2; 0.5 x 0.5 cm^2) using a DISCO DAD 321 automated saw. Before dicing, all wafers were coated with 1.5 μm of photoresist (ref PFR7790EG, from JSR Electronics), which is soluble in acetone, to protect the film surface.

2.2.1.2. Monolayer formation

11-mercapto-1-undecanol ($SH-(CH_2)_{11}OH$; 97%, Aldrich) and 1-hexadecanethiol ($SH-(CH_2)_{15}CH_3$; 92%, Aldrich) were used as received. Pure thiol solutions were prepared in ethanol (Merck, 99.8%) with a final concentration of 1mM. Mixtures of the two thiols, $SH-(CH_2)_{11}OH$ and $SH-(CH_2)_{15}CH_3$, were obtained by mixing the pure solutions in different percentages. All the solutions were prepared in a nitrogen environment inside a glove box. Just before being used, gold substrates were cleaned twice in acetone and immersed in a "piranha" solution (7 parts concentrated H_2SO_4 and 3 parts 30% H_2O_2) for 5 minutes. Substrates were rinsed sequentially with ethanol, water (distilled and deionised) and ethanol

for 2 minutes in an ultrasonic bath. After being blown dry with a stream of argon, gold slides were immersed in the alkanethiol solutions. Incubation was performed at room temperature over 24 hours in a nitrogen environment. After incubation, the monolayers were rinsed three times in fresh ethanol in an ultrasonic bath for 2 minutes. Monolayers were blown dry with a stream of argon and maintained in a container filled with nitrogen until used.

2.2.1.3. Surface characterisation

i. XPS Characterisation of SAMs

XPS measurements were carried out on a VG Scientific ESCALAB 200A (UK) spectrometer using magnesium Kα (1253.6 eV) as radiation source. The photoelectrons were analysed at a take off angle of 55º. Survey spectra were collected over a range of 0–1150 eV with an analyser pass energy of 50 eV. High-resolution C(1s), O(1s), S(2p) and Au(4f) spectra were collected with an analyser pass energy of 20 eV. The binding energy (BE) scales were referenced by setting the $Au_{4f7/2}$ BE to 84.0 eV. All the spectra were fitted using an XPS peak fitting program (XPSPEAK Version 4.1). All the carbon spectra were fitted using asymmetrical 70% Gaussian/ 30% Lorentzian profiles.

The composition of the mixed SAMs in SH-$(CH_2)_{11}$OH was calculated using the O(1s) peak intensity of each mixed SAMs normalised to the O(1s) peak intensity of the SAM prepared from the pure SH-$(CH_2)_{11}$OH solution.

ii. Contact angle Measurements of SAMs

Contact angle measurements were performed with a contact angle measuring system from

Data Physics, model OCA 15, equipped with a video CCD-camera and SCA 20 software. The equipment incorporates an electronic syringe unit with a gas tight 500µl dosing syringe (Hamilton).

SAMs were placed in a closed, thermostatted chamber saturated with the liquid sample in order to prevent evaporation of the liquid from the drop. Measurements were carried out using the sessile drop method, 5 replicates, using 1 drop (distilled and deionised water) for sample at 25ºC were used. After 4µL drop deposition, images were taken every 2 seconds over 600 seconds. Digital images of the drop were stored by the CCD-camera and used for the calculation of the contact angle. Droplet profiles were fitted using different mathematical functions in order to calculate the contact angle. The Young-Laplace method was used to calculate contact angles higher or equal to 90º; the ellipse method was used for contact angles lower than 90º and the tangent method was used for contact angles lower than 30º. The water contact angle for each SAMs was calculated by extrapolating the time dependent curve to zero.

iii. Ellipsometry of SAMs

The ellipsometer is an optical instrument that measures the changes in the polarization of light due to reflection. Ellipsometry was used to measure the thickness of the monolayers. Ellipsometry measurements were performed using an Imaging Ellipsometer, model EP^{102}, from Nanofilm Surface Analysis. This ellipsometer was operated in a polarizer-compensator-sample-analyzer (PCSA) mode (null ellipsometry). The light source was a solid-state laser with a wavelength of 532 nm. The gold plate refractive index (n) and extinction coefficient (k) were determined by using a delta and psi spectrum with a variation of angle between 60

and 75º. These measurements were made in four zones to correct for any instrument misalignment.

To determine the thickness of SAMs, the same kind of spectrum was used and *n* and *k* for the organic layer were set as 1.45 and zero, respectively. Results are the average of 4 measurements on each of the 3 samples for each type of SAM.

2.2.2. Protein adsorption using radiolabelling technique

2.2.2.1. Fibrinogen (HFG) and Albumin (HSA) solutions

Protein solutions were obtained by dissolving HFG (Sigma, ref. F4129) or HSA (Sigma, ref. A1653) in PBS (Sigma, pH 7.4, lot 082k8215), or degassed PBS with 0.01M of NaI – iodinated PBS (PBSI) at a concentration of 0.1 mg/mL. Buffer with iodide (PBSI) was used for radiolabelled tests to avoid the adsorption of free radioactive iodine. This protein concentration is usually used in order to induce the formation of a monolayer of protein, once higher concentrations may promote multilayer adsorption of proteins.[103]

2.2.2.2. HFG labelling with Iodine-125

Quantification of adsorbed HFG on the different monolayers was performed using ^{125}I-labelled HFG. HFG was labelled using the iodo-gen method[104, 105]. Purification of the labelled protein was performed using Sephadex G-25 M columns (PD-10, Amersham Pharmacia biotech). ^{125}I-labelled fibrinogen was added to unlabelled fibrinogen solution in order to obtain a final activity of 10^8 cpm/mg.

2.2.2.3. Quantification of adsorbed HFG to SAMs

To perform HFG adsorption tests, all the SAMs were placed in a 24-well tissue culture plate (Sarsted) with the surface facing up. A small amount of PBSI was added to the periphery of the wells to maintain moisture. A drop of 10 μL of HFG solution was pipetted onto each SAM and the adsorption tests were carried out at 25°C over a 15 min period. After protein adsorption, SAMs were rinsed four times with 2 ml of PBS. The gamma activities were counted with the samples placed in radio-immunoassay tubes. Three replicates were used. The counts from each sample were averaged and the surface concentration was calculated by the equation:

$$HFG\,(\mathrm{mg/m^2}) = \frac{\mathrm{Counts\,(cpm)}.\mathrm{C_{solution}}\,(mg/mL)}{A_{solution}\,(\mathrm{cpm/mL}).\mathrm{SA\,(m^2)}}$$

where the Counts are the radioactivity measurement from the SAMs, the $C_{solution}$ and $A_{solution}$ are the concentration and the specific activity of the protein solution, respectively, and SA is the surface area of the drop. Surface area of the drop (SA) was calculated using the drop surface contact diameter obtained using the contact angle measuring system software described below, for the same conditions used during the protein adsorption test (10 μL of HFG solution, 0.1 mg/mL, 25ºC and 15 min.). Sigal et al[64] demonstrated that an adsorption time of 15 minutes is enough to reach an adsorption plateau on SAMs with different functional groups, namely -OH and -CH_3, for protein concentrations of 0.1mg/mL.

2.2.2.4. Competitive adsorption between HFG and HSA to SAMs

For competitive adsorption of HFG in the presence of albumin, the concentration of ^{125}I-HFG

was 0.1 mg/mL and the concentration of unlabelled HSA was 0.1 mg/mL and 1 mg/mL. Calculations were performed considering as 100% adsorption the concentration of HFG adsorbed using a pure fibrinogen solution.

2.2.2.5. Exchangeability of adsorbed HFG with other proteins in solution

Exchangeability tests were carried out immersing the labelled SAMs over 24 hours in an unlabelled HFG pure solution (1 mg/mL, 25ºC) or a human serum albumin (HSA) pure solution (1 mg/mL, 25ºC). The samples were then washed with the buffer and their residual radioactivity counted.

2.2.3. Platelet adhesion and activation

Platelet adhesion to the different SAMs was assessed using SEM. The effect of the pre-immersion of the SAMs in an albumin solution on platelet adhesion and activation was evaluated. In order to complement these studies in future work, other techniques, as Wright staining, Glutaraldehyde Induced Fluorescence Technique (GIFT) and Flow Cytometry were optimized using gold substrates.

2.2.3.1. Preparation of platelet rich plasma (PRP)

Blood from healthy donors denying any medication for at least 10 days was collected and processed at the Portuguese Institute of Blood (IPS). Whole blood (plasma, platelets, leucocytes and erythrocytes) was obtained directly from the bags that contain anti-coagulant. Buffy Coat (platelets and leucocytes) was obtained by centrifugation of the total blood unit at

3900 rpm 10 minutes at 22ºC. PRP is the supernatant obtained by centrifugation of the buffy coat at 1000 rpm for 10 minutes at 22ºC. PRP rested for 1 hour and after was stored at 22ºC with constant agitation. Two different concentrations of PRP (2 x 10^8 and 4 x 10^8 platelets/ml) were prepared and counted using a haematology analyzer (Cell Dyn 3700 system from Abbott Diagnostic Division).

Basal platelets activation and activation of platelets induced by the platelet antagonist thrombin (0.35U/ml) were studied as control for platelets functionality.

2.2.3.2. Quantification of adhered platelets to SAMs and gold substrate

Each SAM and gold substrate was attached to the bottom of a large diameter piece of Silastic™ tubing and placed into a 24 well plate (Sarstedt; ref. 83.1836.500). Special care was taken to ensure the creation of an airtight seal between the SAM and the tubing that fits snuggly into the well. 200 μl of PBS was added to each well for 15 min at room temperature and then removed. To evaluate platelet material interactions, 200 μl of freshly prepared PRP (3 x 10^8 platelets/ml) was added to each well. The 24 well plate was sealed with parafilm and incubated for 30 min at 22.4ºC in a horizontal shaker (Platelet incubator from Helmer – model PC 3200 series 300996K) at 70 rpm. 100 μl of supernatant were removed from each well and subjected to flow cytometry analysis. The remaining supernatant was removed and the wells were rinsed 3x with 600 μl PBS to remove residual PRP.

i. Scanning electron microscopy (SEM)

Adherent platelets were fixed with a freshly prepared solution of 1.5% Glutaraldehyde (Merck 4239, ref R1011; 25%; Agar; Mw=100.12 g/mol) in 0.14M sodium cacodylate (BDH 30118;

Merck, ref 1.03256.0100; Mw=214.05g/mol) buffer for 30 min at room temperature. After being rinsed twice with PBS and dehydrated with an increasing ethanol (99%)/water gradient, samples were maintained for 10 minutes in each of the following solutions: 50%, 60%, 70%, 80%, 90% and 99%. Finally, hexamethyldisilazane (C6H19NSi2; Sigma, ref H4875; Fw 161.4) was added to each sample and they were left to dry on the hoot over night (without the cover).

ii. Wright staining

Adherent platelets were fixed with the following solution: Formol 40%, H_2O, NaH_2PO_4, Na_2HPO_4. Samples were glued into microscope slide and placed in staining jars with:

1 Hemacolor 2, colour reagent red (1.11956.2500, Merck) for 2 minutes

2 Hemacolor 3, colour reagent blue (1.11957.2500, Merck) for 1 minute

Slides were rinsed with tap water and dried with a hair dryer.

iii. Glutaraldehyde Induced Fluorescence Technique – GIFT

Adherent platelets were fixed with a freshly prepared solution of 1.5% glutaraldehyde in PBS buffer for 30 min at room temperature. Samples were rinsed three times with PBS and once with deionized water and placed in regular microscope slides. One drop of fluorescent mounting medium (Vectashield – H-1000; Vector Laboratories, Inc) was added and a coverslip was placed on the top of each sample. Platelets were visualized with a fluorescence microscope (Axiovert). The fluorescence (epifluorescence) was stimulated with light (wavelengths 450 to 490 nm) and the emission detected at 515 nm. The numerical aperture of the objective lens (40x) was 0.7 with a calculated maximal optical resolution of 0.37 μm.

iv. Flow cytometry – FC

In order to identify the platelet population and its activation, before and after contact with the different samples, two fluorescent markers were used: CD61-PercP (BD) for platelet counting and CD62-PE (BD) to detect platelet activation. These markers are detected by flow cytometry, using specific antibodies conjugated with fluorescein (FITC) or ficoeritrine (PE) on the several platelet samples.

PP tubes with 100 µl of supernatant and tubes with 100 µl of original platelet concentration (3 x 10^8 platelets/ml) received 5µl of a solution of Tyrode buffer and trombin. Platelet solutions (PS) were prepared. The tubes were covered, folded once and then 25 µl of PS are removed from each PP tube to another PP tube (each sample has 2 tubes: 1 to study basal activation and 1 to study thrombin activation). Finally, the addition of the fluorescent markers was done: 5 µl of CD61 and 5 µl of CD62 to each tube (basal and trombin). Following 15 min, 5 µl of thrombin (concentration: 0.35U/ml) was added to each trombin tube. Samples were kept in the dark until the 15 min were completed. 1 ml of tyrode buffer was placed in BD Trucount tubes and stired. Analyses by flow cytometry were performed.

3. Results and discussion

3.1. Intervertebral disc substitutes

3.1.1. Attenuated Total Reflection - Fourier Transform Infra-Red spectroscopy (ATR-FTIR)

Figure 15 shows the characteristic spectrum of unmodified PET, in comparison with the modified material. Using this technique, no detectable changes were observed as a result of any of the treatments performed. The depth of penetration is not enough to be detected by the ATR-FTIR analyses. The spectrum obtained for unmodified PET is similar to those reported in the literature.[106]

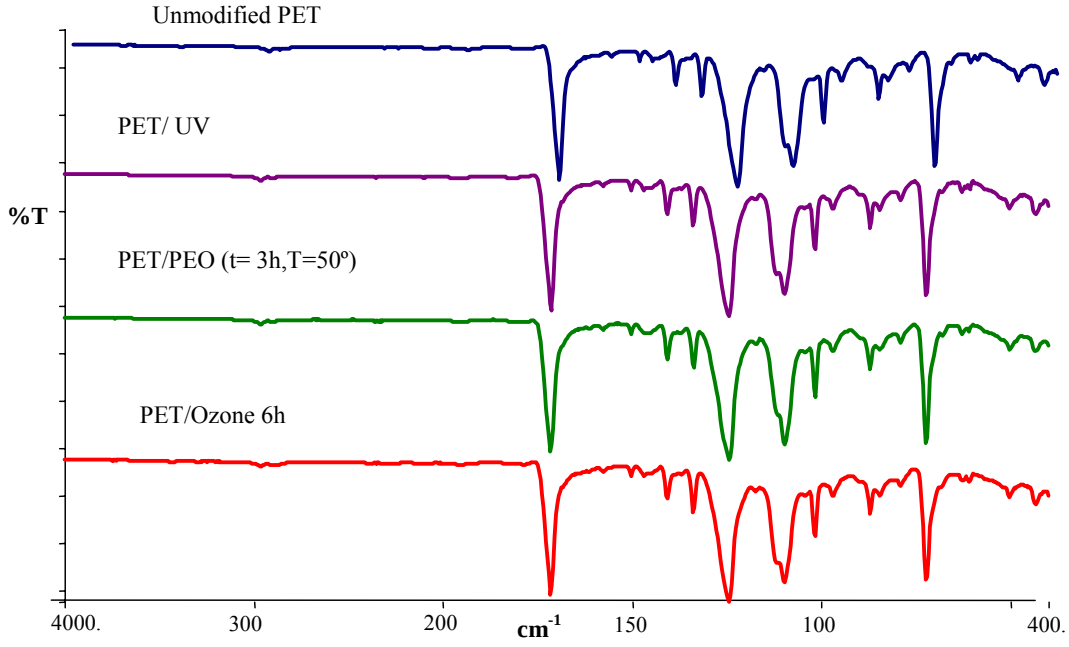

Figure 15 - ATR-FTIR spectrum of untreated and treated PET.

3.1.2. X-ray photoelectron spectroscopy (XPS)

As we observed by the XPS analyses, the survey spectrum (Figure 16) shows that C and O were present in the film, and that there is no contamination. The spectrum is similar to typical XPS spectra obtained for PET.[107]

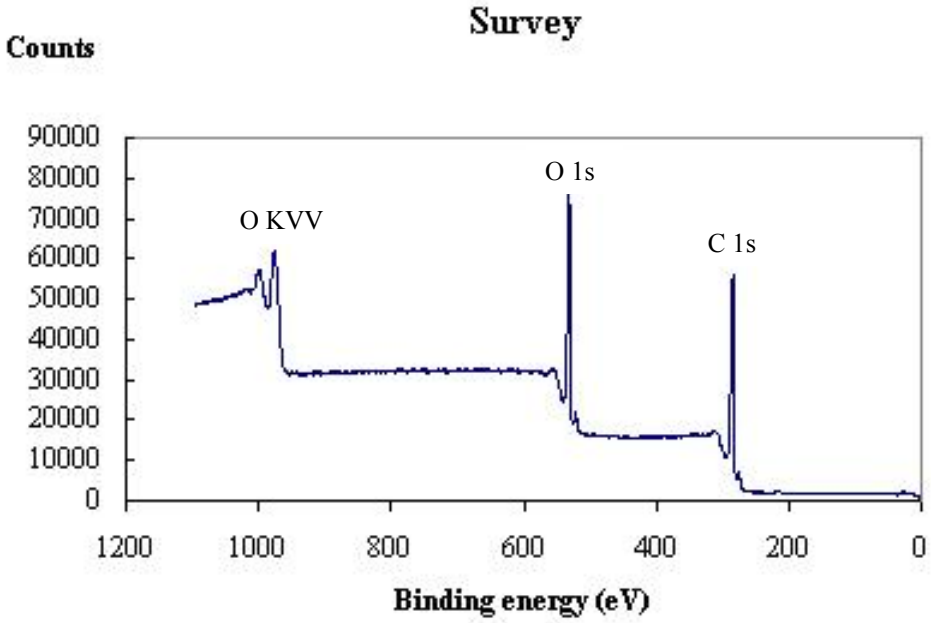

Figure 16 - Survey spectra of PET film

The expected C (1s) and O (1s) peaks were observed in all the samples examined. The atomic percentage of carbon and oxygen obtained by high resolution XPS spectra were 74.1% of C and 25.9% of O, and they were close to the values expected for this polymer (71.5% of C and 28.5% of O).

The primary components of C1s spectrum correspond to the carbon atoms of phenyl ring (C-C, 284.7 eV), methylene carbon atoms (C-O, 286.2 eV) and to the ester carbons (O-C=O, 288.6 eV). The experimental intensity ratio of these three primary components was 61:16:23 (the expected stoichiometry was 60:20:20).

Table I - Atomic percentage of carbon and oxygen species present, obtained by deconvolution of high resolution XPS spectra

Peak (Binding energy)	Atomic (%) observed	Atomic (%) expected
C-C (284.7 eV)	61	59
C-O (286.2 eV)	16	22
O-C=O (288.6 eV)	23	19
O-C (531.5 eV)	38	47
O=C (533.1eV)	62	53

In Figures 17 and 18, we can observe the C1s and O1s peaks. The result from XPS analysis of the untreated PET film and of the PET film washed with ethanol were the same. These spectra are similar to those reported in the literature, confirming that the PET film has no contaminants.

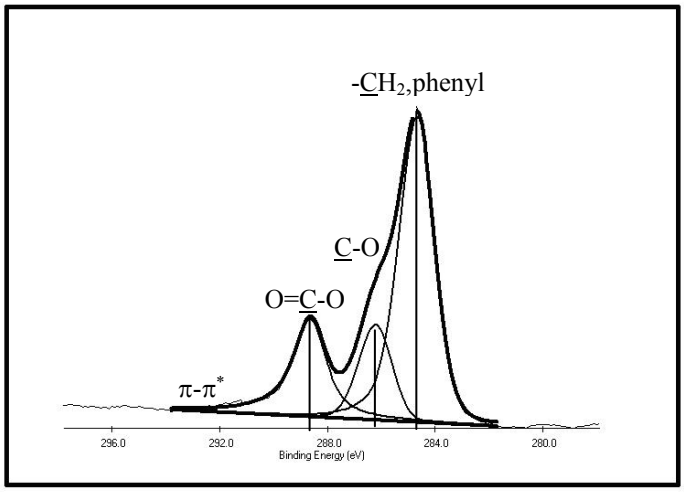

Figure 17. C 1s peaks of PET film

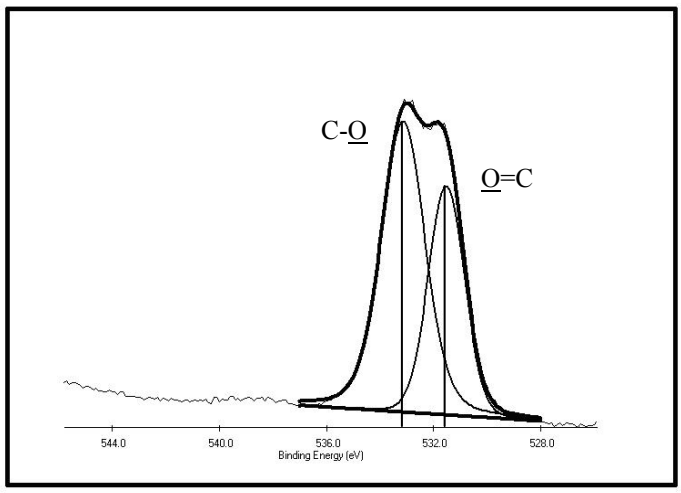

Figure 18. O 1s peaks of PET film

The O1s signal of PET is characterized by a doublet peak correspondent to the singly-bound (533.1 eV) and doubly-bound oxygen (531.5 eV) species as well by a low intensity satellite peak at 538.0 eV assigned to the shake-up satellite structure. Each of these doublet peaks would be expected to have equal intensity to reflect the PET structure; however, the intensity of the peak at 533,1 eV is more intense and larger than the one at 531.5 eV. This is explained by the stronger π-interaction of the carbonyl oxygen with the conjugated system of the phenyl ring.[108]

3.1.3. Contact angle measurements of PET films

Water contact angle data of PET film surfaces, using the sessile drop technique, are reported in Table II. Regarding unmodified PET surfaces, the water/air contact angle of PET varies between 73º and 78º as reported in the literature.[109]

Table II - Water contact angles of different treatments of PET samples

PET Treatment	Contact angle (º)
Unmodified	74.0 ± 2.2
UV radiation	77.0 ± 2.2
Ammonium Cerum IV	72.5 ± 0.6
SPINs of PET and PEO (3 h, T_{amb})	69.4 ± 2.5
SPINs of PET and PEO (3 h, T=80ºC)	69.1 ± 2.1
Ozonation (40 min)	69.7 ± 2.2
Ozonation (6 hours)	38.2 ± 2.2

As the ozonation treatment has shown an increase of hydrophilicity, the effect of incubation in water was studied. Values shown in Table III correspond to unwashed and washed ozone treated PET films using different periods of time. Walzak et al[90] described that surface-oxidation treatments can generate a water-soluble surface consisting of low-molecular-weight oxidized material (LMWOM). These water-soluble components complicate the interpretation of wettability measurements made on ozonated samples.

Table III - Water contact angles of unwashed and washed ozonated PET samples.

Ozonation time (h)	Contact angle (º)	
	Unwashed	Washed
Unmodified	74.0 ± 2.2	---
0.3	64.5 ± 0.4	71.4 ± 0.8
0.7	65.0 ± 1.9	73.2 ± 0.8
1	59.3 ± 1.8	73.3 ± 2.2
2	42.1 ± 2.9	64.5 ± 1.1
3	57.5 ± 2.8	62.8 ± 0.6
5	54.2 ± 5.5	58.5 ± 3.1
6	**38.2 ± 2.2**	**52.3 ± 3.1**

As can be observed, washed films present higher contact angle compared to unwashed ones, which suggests that the formation of LMWOM in the surface is decreasing the contact angle. When measuring the contact angle of any of the ozonated PET samples, dissolution of LMWOM is likely to alter the localized surface tension of the water. In addition, the surface energy of the LMWOM itself may be different from the insoluble underlying material.[90] The best result of ozonation treatment is observed for periods of 6 hours. The contact angle decreases from 74º (unmodified film) to 38.2º (unwashed films) and to 52.3º (washed films).

Contact angle measurements of both sides of ozonated PET samples were performed in order to evaluate the homogeneity of the treatment. Values shown in Table IV correspond to both sides of ozone treated PET films.

Table IV - Water contact angles of both sides of washed ozonated PET samples.

Ozonation Time (h)	**Contact angle (º)** Side 1	Side 2	Average of both sides
0	75.2 ± 3.6	67.5 ± 2.0	71.4 ± 4.9
0.3	74.6 ± 2.7	66.0 ± 1.4	70.3 ± 5.0
0.7	74.2 ± 0.9	69.4 ± 2.6	71.8 ± 3.1
1	72.9 ± 1.1	61.0 ± 1.8	67.0 ± 6.5
2	49.6 ± 3.4	61.7 ± 2.7	55.7 ± 7.0
3	67.7± 2.6	62.8 ± 0.6	65.2 ± 3.1
5	67.4 ± 1.4	61.0 ± 1.3	64.2 ± 3.6
6	52.3 ± 3.1	50.9 ± 7.2	51.6 ± 5.0

In this Table we can observe that ozonation treatment was not homogeneous process showing differences between both sides of the same film.

3.1.4. Scanning electron microscopy of PHEMA/ozone modified PET single fiber samples

Figure 19 shows SEM micrographs of PHEMA/PET fiber samples after tensile strength tests. PET fibers used were coated with PHEMA right after the ozone treatment.

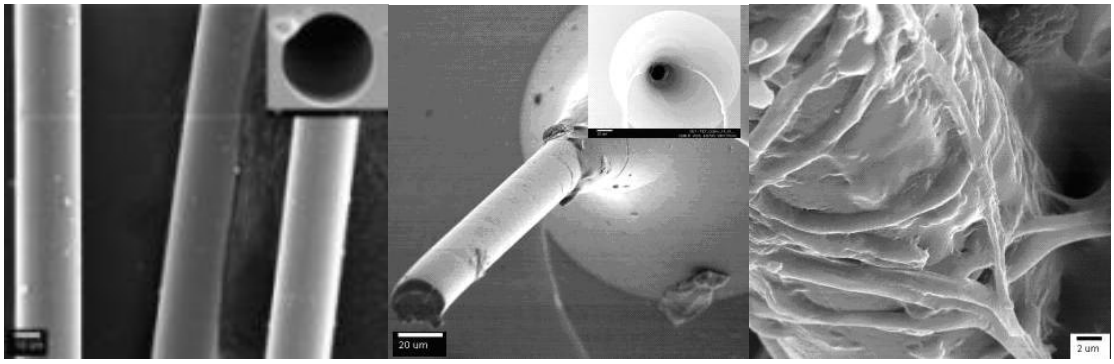

A B C

Figure 19. SEM micrographs of ruptured PHEMA/PET fiber samples. a) Unmodified PET fiber, b) PHEMA hydrogel reinforced with PET fiber ozonated for 6 h. c) PHEMA hydrogel reinforced with PET fiber ozonated for 6 h, and immersed in PHEMA reactive solution.

SEM micrographs confirmed that the best adhesion between modified PET fiber and PHEMA hydrogel matrix was obtained when PET fibers were immersed in PHEMA solution. In this case, the PHEMA coating the fiber can be observed in Figure 19.

The analysis of other mechanically tested samples has shown that all other treatments promoted a poor adhesion between the fiber and the matrix, which was evidenced by holes left in the matrix after the fibers were pulled-out.

In Figure 20 SEM micrographs of PHEMA/PET bundles samples after tensile strength tests can be observed.

The analyses of tested samples has shown that PET bundles without any treatment promoted poor adhesion between the PET bundles and the PHEMA hydrogel matrix, which was evidenced by round holes around the PET bundles (Fig.20A).

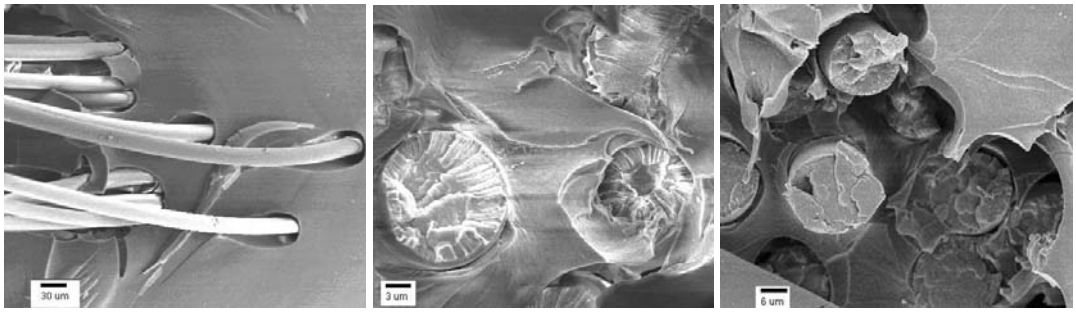

A B C

Figure 20. SEM micrographs of ruptured PHEMA/PET bundles samples. a) Unmodified PET bundles, b) PHEMA hydrogel reinforced with PET bundles ozonated for 6 h. c) PHEMA hydrogel reinforced with PET bundles ozonated for 6 h, and immersed in PHEMA reactive solution.

SEM micrographs of PET bundles ozonated for 6 hours have shown that this treatment promotes good adhesion between PET bundles and PHEMA hydrogel matrix (Fig.20B). PET bundles used were immersed in a PHEMA reactive solution right after the ozone treatment. SEM micrographs confirmed that the best adhesion between modified PET bundles and PHEMA hydrogel matrix was obtained when PET bundles were immersed in PHEMA solution (Fig.20C). In the latter case, a strong bonding between PET and PHEMA was found, since the fractured fibers pulled some matrix together.

3.1.5. Mechanical characterization

3.1.5.1. Tensile strength of PET monofilaments

The strength of fibers can exhibit variations of 30% around the average value. Therefore, it is important to describe the mechanical properties of fibers through a distribution function, the Weibull distribution.[110] To evaluate the fiber strength it is necessary to have a mathematical model describing the fracture of fibers.

Weibull parameters of the strength distribution, α (the shape parameter) and β (the scale parameter) and tensile strength average,[111] for the single fibers are obtained by the measurement of the tensile strength on the Instron. For the statistical treatment, Kaleida software was applied.

The experimental data were fitted by the Weibull cumulative distribution function defined as:

$$F(l)=1-\exp\{-[(l/\beta)^{\alpha}]\}$$

Where F(l) is the cumulative probability for fragments of length *l*.

The Weibull theory is a statistical data treatment of the tests performed.

In figures 21 and 22 the frequency-stress graphs for 30 and 40 mm can be observed. The graphs describe the probability for the fibers to break at a definite stress value. The most probable value is the one corresponding to a frequency of 0.5.

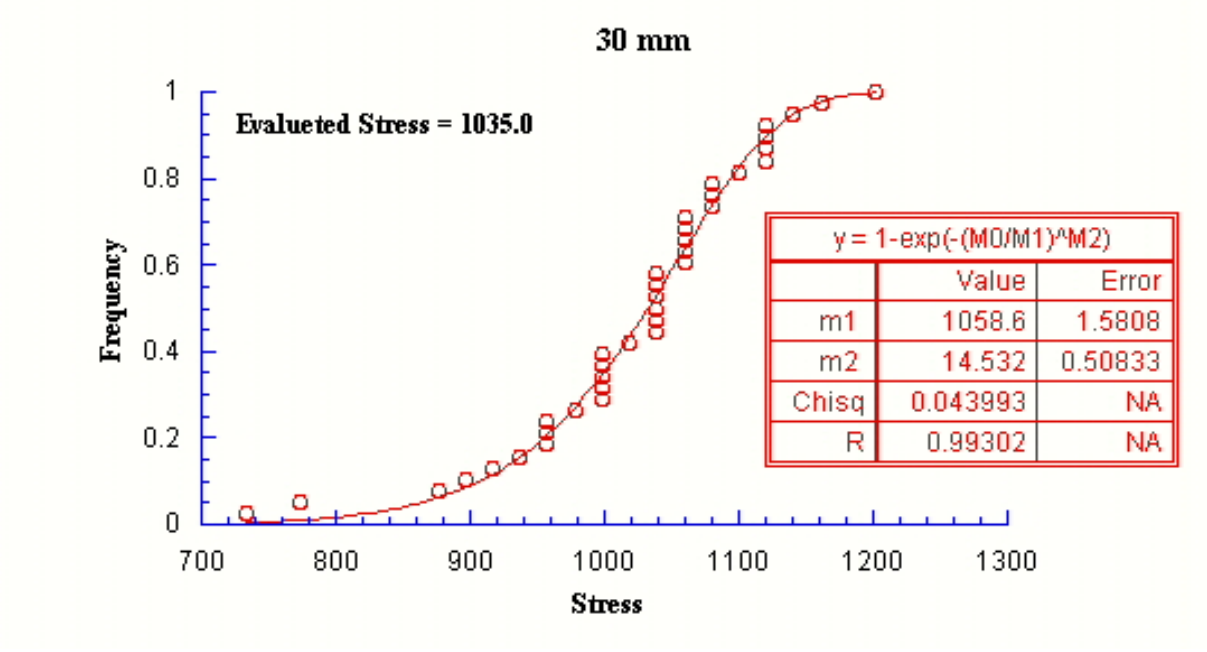

Figure 21. Weibull distribution of single PET fiber with 30mm length

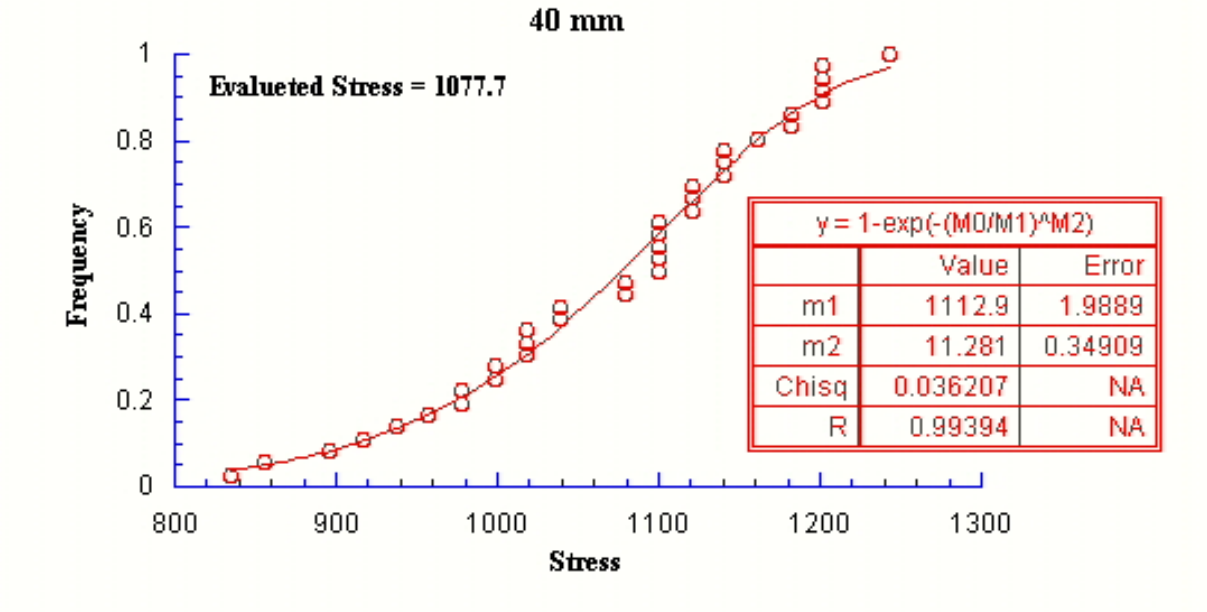

Figure 22. Weibull distribution of single PET fiber with 40mm length

3.1.5.2. Tensile strength tests with PHEMA hydrogels reinforced with ozone-treated PET monofilament

Figure 23 displays the maximum stress of PHEMA hydrogels reinforced with ozone-treated PET monofilaments (diameter of 0.025 mm) using different methodologies. The results show that the maximum stress of PHEMA hydrogel reinforced with PET monofilament ozonated for 6 h (bar B) is higher than the one achieved for PHEMA hydrogel alone (bar A). However, care must be taken in the interpretation of the results since the standard deviation is large (~ 0.06).

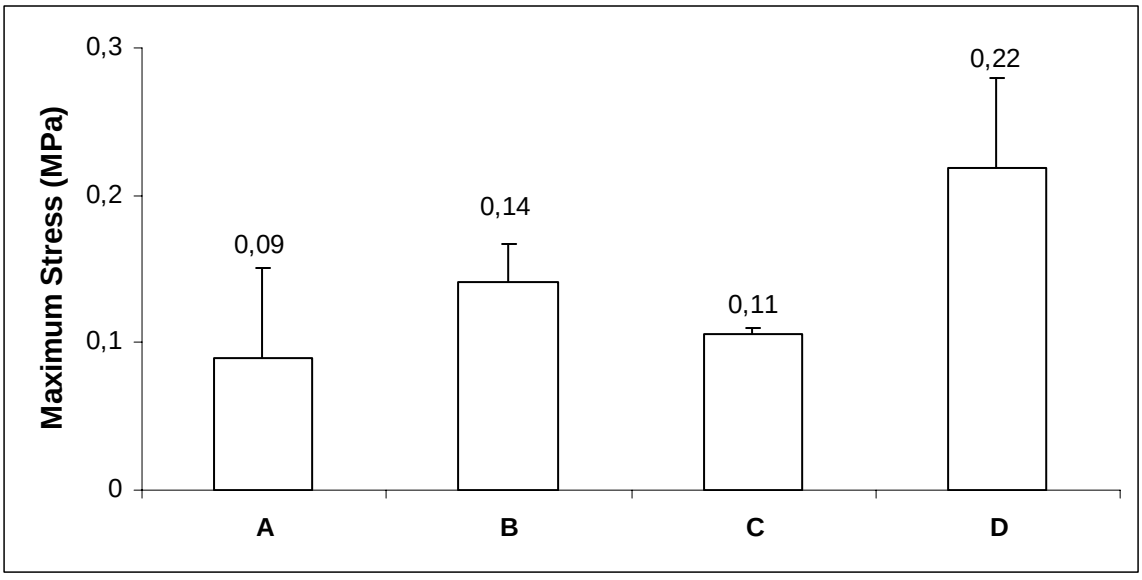

Figure 23. Tensile strength tests of PHEMA/PET samples. A) PHEMA hydrogel (negative control); B) PHEMA hydrogel reinforced with PET monofilament ozonated for 6 h; C) PHEMA hydrogel reinforced with PET monofilament ozonated for 6 h, coated with HEMA reactive solution and then cured at 80ºC for 2 h; D) PHEMA hydrogel reinforced with PET monofilament ozonated for 6 h, and coated with HEMA reactive solution (no curing).

When the ozonated PET monofilament was immediately coated with HEMA and cured before preparing the sample, the mechanical properties were further lowered (bar C) probably due to the fact that a new interface was introduced, along which the sample fails. However, when the ozone treated and HEMA-coated PET fibers were introduced in the PHEMA matrix, without being previously cured, it resulted in a sample with improved mechanical properties (bar D), compared to the original PHEMA alone. In this case, it seems that a homogeneous sample was prepared.

It should be noted that the maximum stress of PET monofilament in the absence of PHEMA hydrogel is 0.02 MPa. Therefore, the maximum stress for PHEMA hydrogels reinforced with PET monofilaments should be close to the value obtained for PHEMA hydrogel alone.

In order to increase the sensitivity of the measurements, bundles replaced the monofilaments in the next experiments.

3.1.5.3. Tensile strength tests with PHEMA hydrogels reinforced with ozone-treated PET bundles

A fiber-reinforced composite consisting of continuous fibers of PET fibers and PHEMA hydrogel matrix phases exhibits the uniaxial stress-strain response illustrated in Figure 24 (the mechanical response of PET fibers and PHEMA hydrogel is additionally displayed). The Stage I of the curve is linear which means that either PET fibers or PHEMA matrix deform elastically. In this type of composite, the matrix yields and deforms plastically while the fibers continue to stretch elastically, whereas the tensile strength of the fibers is significantly higher than the yield strength of the matrix.

Composite failure is not catastrophic for several reasons. First of all, not all the fibers fracture at the same time, since there will always be considerable variations in the fracture strength of brittle fiber materials. In addition, even after the fiber failure, the matrix is still intact. Thus, these fractured fibers are still embedded within the intact matrix, and consequently are capable of sustaining a diminished load as the matrix continuous to plastically deform.

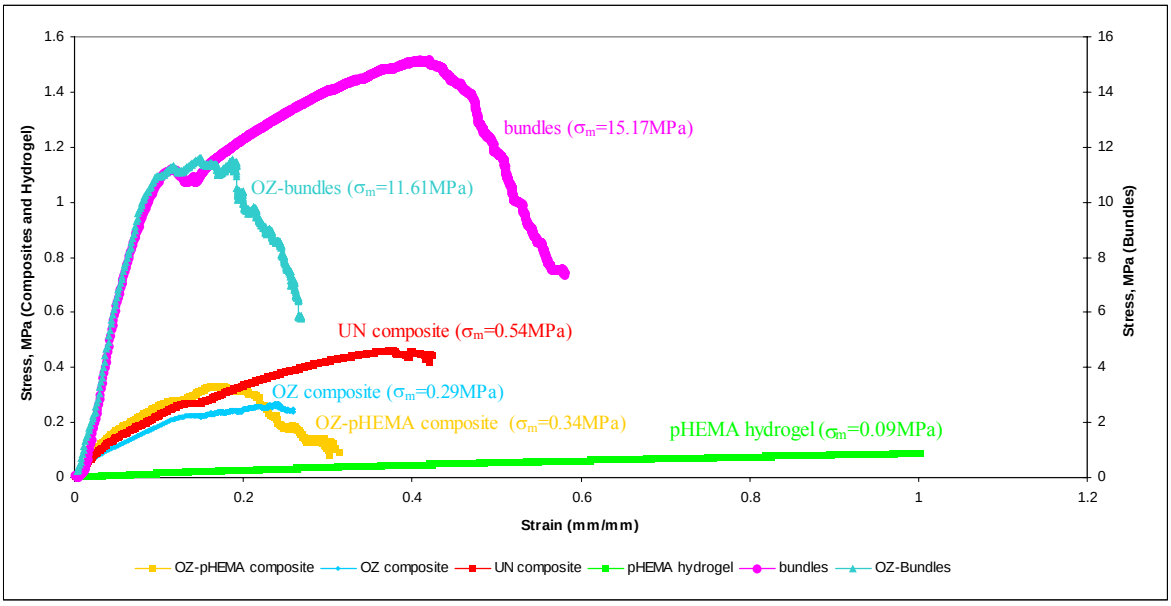

Figure 24. Mechanical tests of PHEMA/PET fibers composites (for details about the samples see section 2.1.4.).

The stress obtained for PHEMA hydrogels without any reinforcement with PET fibers is ca. 0.09 MPa. The incorporation of untreated PET fibers (diameter of 0.75 mm) into PHEMA hydrogels increases ca. six times the stress (Fig.24 and Fig.25).

Figure 25 represents the maximum stress and maximum strain of PHEMA hydrogel and PHEMA hydrogel reinforced with PET fibers composites.

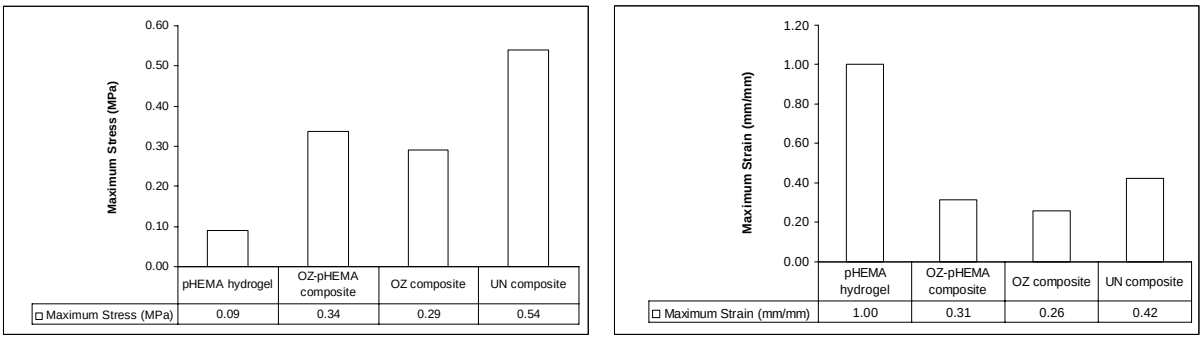

Figure 25. Maximum Stress and maximum strain of PHEMA hydrogel and PHEMA/PET fibers composites (for details about the samples see section 2.1.4.).

During the tensile tests most of the hydrogels (65%) are broken in the vicinity of the clamps and the PET fibers remain intact and sweep from their interior (see Fig.26A in next page). This data suggests that the adhesion between untreated PET fibers and PHEMA hydrogel is reduced.

When the ozone-treated PET fibers were incorporated into PHEMA hydrogels, the maximum stress obtained in these composites was lower than the maximum stress obtained with composites of untreated PET fibers (Fig.26). However, the fiber-matrix interfacial bond is very good, showing interaction and adhesion between the components. Furthermore, most of the tests (83.3%) ended by the breakage of the bundle in the middle of the sample, in contrast to the results obtained previously. In addition, the PET fibers that remained in the hydrogel are clearly adhered to the PHEMA hydrogel (Fig. 26B).

Ozone-treated PET fibers are degraded by ozone treatment and therefore their mechanical performance is lower. To clarify this issue, ozone-treated (6h) and untreated PET fibers were mechanically characterized regarding their tensile properties. The maximum stress obtained was 15.17 ± 3.1 MPa (corresponding to a maximum force of 6.67 N) and 11.61 ± 2.01MPa (5.12 N) for untreated and ozone-treated PET fibers, respectively.

In PHEMA hydrogels reinforced with PET fibers (ozonated for 6 h and swollen overnight in HEMA reactive solution) the maximum stress value (0.34 MPa) is close to the value obtained in PHEMA hydrogels reinforced with ozone-treated PET fibers (0.29MPa). However, this value is lower than the one obtained for PHEMA hydrogels containing untreated PET fibers (0.54MPa). Similarly to the results present in the previous paragraph, in most tests (61.5%) the fibers have broken in the middle of the sample (Fig.26C).

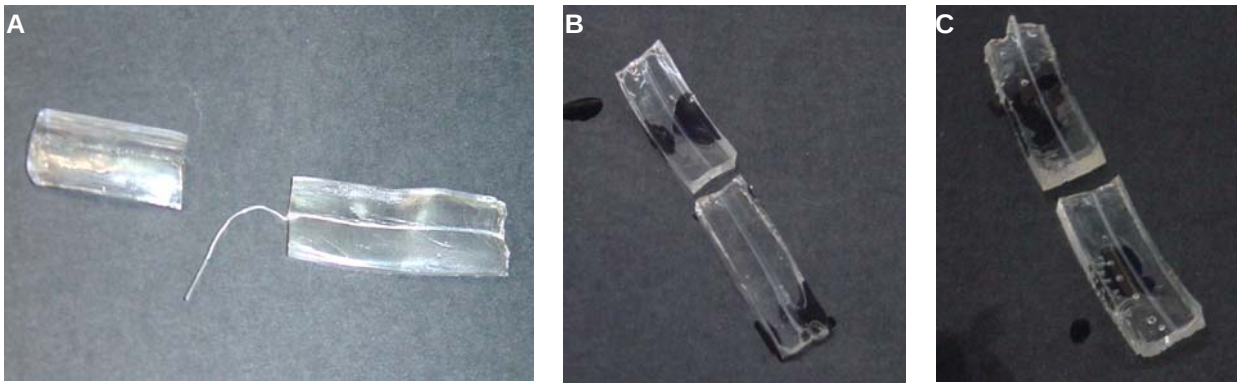

Figure 26. Photographs from PHEMA/PET samples after tensile tests. A) PHEMA hydrogel reinforced with untreated PET fibers; B) PHEMA hydrogel reinforced with PET fibers ozonated for 6 h; C) PHEMA hydrogels reinforced with PET fibers ozonated for 6 h and swelled overnight in HEMA reactive solution.

3.2. Blood contact devices

3.2.1. Surface characterisation of gold

Gold substrates were characterised by XPS and contact angle measurements after being cleaned with "piranha solution" and before immersion in the thiol solutions.

No sulphur was detected on these surfaces. As described by Martins et al.[1] carbon and oxygen were always present on the gold samples. Several authors have found that, although gold is

inert compared with other metals, the surface is nevertheless of high free energy, and under ambient laboratory conditions is covered with a reversibly physiosorbed layer of water, hydrocarbons and other organic compounds. Bain et al.[76] have observed that the water contact angle of these surfaces can change from 30º to 70º compared to the 0º reported for clean gold.[70] Furthermore, within some minutes of exposure to the laboratory atmosphere, a clean hydrophilic gold surface is rendered hydrophobic by adsorption of nonpolar contaminants. XPS indicates the presence of non-volatile carbon- and oxygen–containing contaminants on its surface.[78, 112] However, after 24 hours of immersion in the thiol ethanolic solutions, the effect of the carbon or oxygen contaminant layers on the gold surface is insignificant.[112]

3.2.2. Surface characterization of SAMs

Three different SAMs were prepared and characterized in order to verify if they were in accordance with the previous work performed by Martins et al.[1] Pure SAMs of SH-$(CH_2)_{11}OH$ (100% C11OH) and SH-$(CH_2)_{15}CH_3$ (0% C11OH) and mixed SAMs prepared using a solution of these two alkanethiols (90% C11OH) were analysed by XPS, contact angle measurements and ellipsometry.

For all SAMs studied, no chemical element other than the ones expected, based on their chemical configuration, were noticed in XPS survey spectra, as demonstrated in Figure 27.

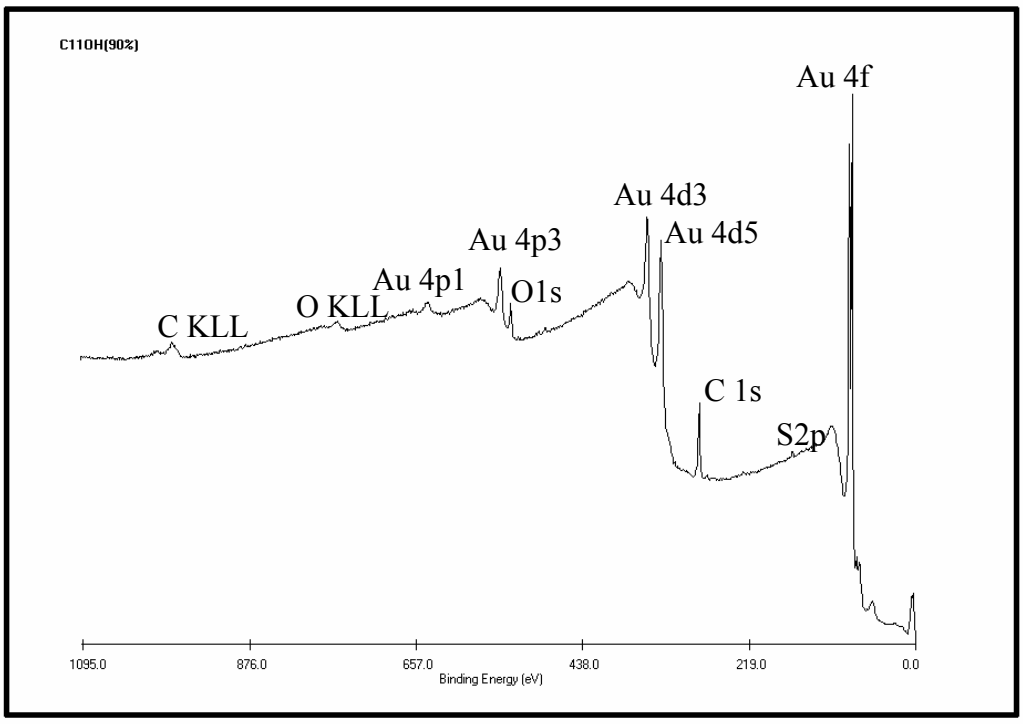

Figure 27. XPS survey spectra of 90% C11OH SAMs.

Figure 28 shows the atomic percentages of carbon, oxygen and sulphur of the three different SAMs prepared determined by XPS.

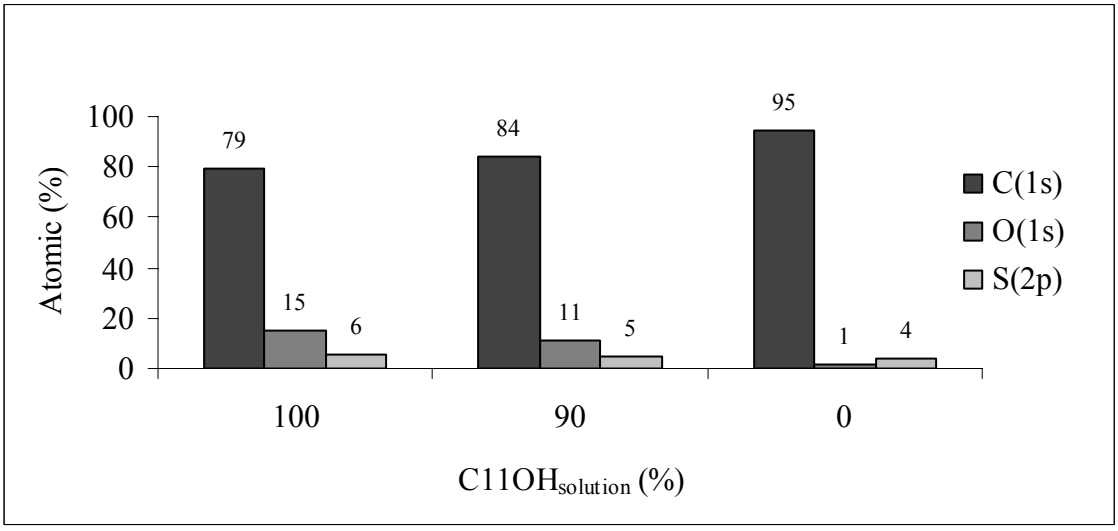

Figure 28. Relative atomic composition (%) of SAMs prepared from mixtures of C11OH and C15CH3 dettermined by XPS (take-off angle of 55º)

This figure shows that there is a decrease of oxygen and an increase of carbon and sulphur with a decrease of the percentage of C11OH. The difference between chain length (n =11 and n =15) of the two alkanethiols used may explain the decrease of the sulphur (attenuantion of the buried sulphur signal).

In some samples prepared from a solution of C15CH3 a residual peak of oxygen, which was described by other authors,[113,114] has been detected.

Figure 29 shows the C1s, O1s, S2p, and Au 4f XPS spectra of a mixed monolayer adsorbed from a mixture of 90% C11OH and 10% C15CH3.

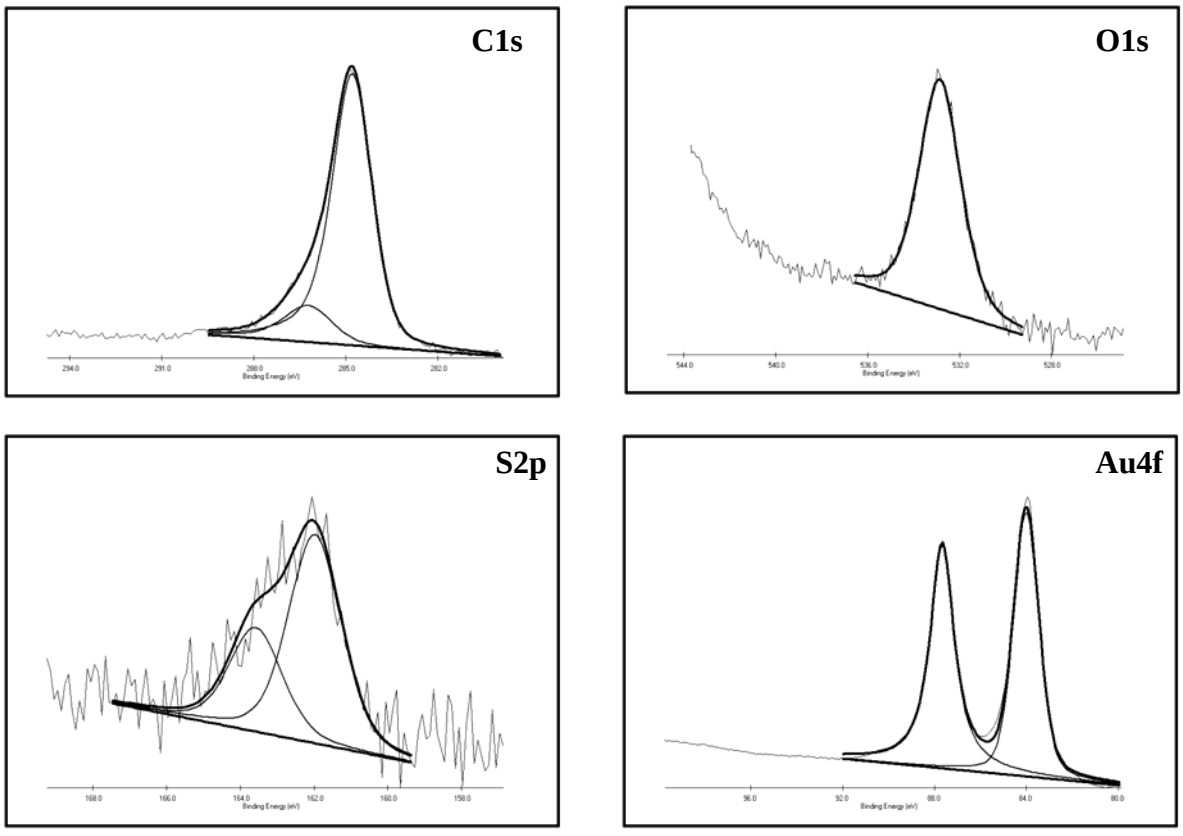

Figure 29. Spectra of XPS (C1s, O1s, S2p, and Au 4f) of 90% C11OH SAMs.

XPS high resolution spectra of the C1s, O1s, S2p, and Au4f of a mixed monolayer adsorbed from a mixture of 90% C11OH and 10% C15CH3 are in accordance with results reported by

other authors.[115] The C1s binding energy of the mixed SAMs, centred at 285 eV, corresponds to the C-C and C-H bond in the alkanethiol. The additional C1s peak, centred at 286.7 eV, corresponds to the C-O bond, from the OH- groups present on the monolayer.

The O1s binding energy was centred at 532.8 eV and Au 4f was centred at 84 and 87.7 eV.

The sulphur high-resolution spectra of these SAMs were obtained with a doublet structure centred at 162 and 163.2 eV and a peak area ratio of 2:1, being in agreement with described by Castner et al (162.1 and 163.3 eV).[114]

In figure 30 the contact angles of the SAMs prepared from mixtures of C11OH and C15CH3 are given. It is visible that the hydrophilicity of the SAMs increases linearly with the incorporation of C11OH thiol in the monolayer, as described elsewere (18.1±1.6; 44.0±0.8; 106.7±1.3).[1]

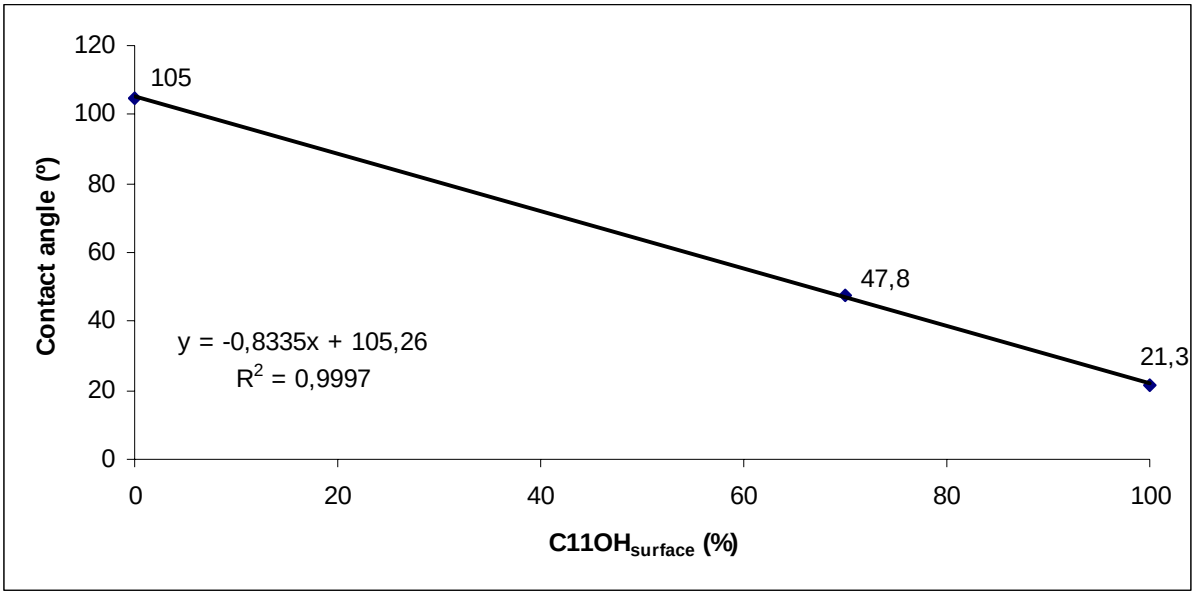

Figure 30. Contact angle (º) versus percentages of OH groups on the surface of SAMs prepared from mixtures of C11OH and C15CH3.

Surface characterization of these SAMs using XPS and contact angle measurements are in accordance with described by Martins et al.[1] Concerning SAM preparation, their surface concentration is not equal to the composition of the thiol solutions, since there is a strong preference for the adsorption of the longer and methyl-terminated thiol. In this previous investigation performed in our laboratory, it was described that thiol solutions with 80% and 90% of C11OH give a percentage of OH groups on the surface of the monolayer of about 36 % ± 9 and 65% ± 6 respectively. In this work, several surface concentrations of C11OH (0%, 36%, 65% and 100%) have been studied in order to have a gradient of functionalities on the surface.

Ellipsometry was applied as a precise technique of determining the average monolayer thickness of the pure and mixed SAMs prepared from solutions of C11OH and C15CH3.

As can be observed in Figure 31 the thickness of the films decrease linearly as the concentration of OH increases.

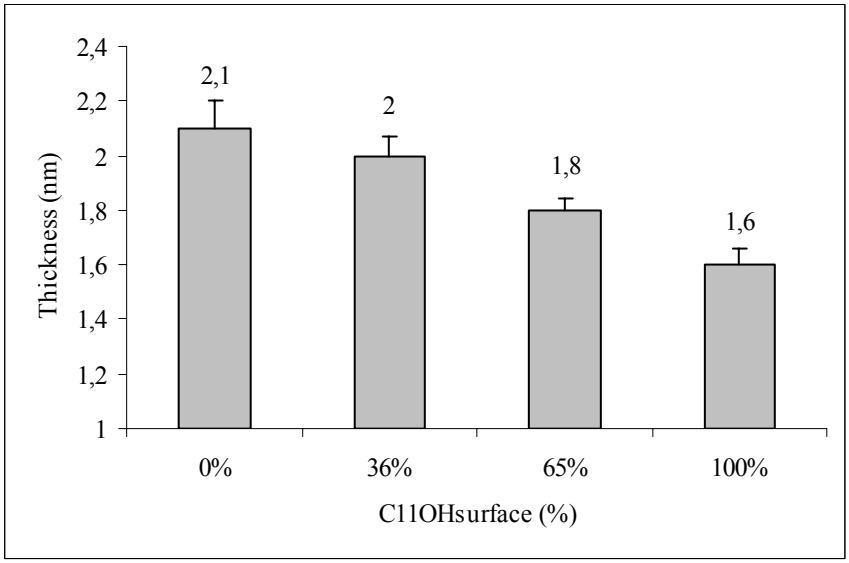

Figure 31. Film thickness of SAMs prepared frompure and mixtures of C11OH and C15CH3.

Monolayers assembled by n-alkyl thiols ($CH3(CH2)_nSH$ where n=1,3,5,7,9,11,15,17, and 21), adsorbed on gold from dilute solution, have been characterized by optical ellipsometry by Porter et al.[115] They report that there are distinct differences in the thickness of the SAMs between long- and short-chain thiol monolayers. Their ellipsometric data indicated that long chain thiols ($CH_3(CH_2)_{n>9}SH$) tilted by 20-30º from the surface normal. If an average tilt of 25º is introduced, a slope of 0.11 nm per CH_2 group and an intercept of 0.51 nm result. Extrapolating this equation to our layers with 100% C11OH SAMs, which have 11 CH_2 groups, a thickness of 1.7 nm is expected, theoretically. The thickness obtained was 1.6 nm, which is close to the theoretical value. Concerning our layers with 0% C11OH, which have 15 CH_2 groups, they should have, in theory, a thickness of 2.16 nm. The result obtained is very similar (2.1 nm). Mixed SAMs should have thickness values between 1.6 and 2.16 nm, which has been confirmed by our results.

3.2.3. Protein Adsorption

3.2.3.1. Quantification of HFG adsorption on different SAMs

HFG adsorption obtained using ^{125}I-labeled HFG on the different SAMs is shown in Figure 32. The contact drop diameter used in the calculations of the surface area ranges from 3.7 to 5.0 mm depending on C11OH percentage on the SAMs surface.

Pure C15CH3 SAMs produced the highest HFG adsorption. The concentration of HFG on this monolayer was 6.7 ± 0.8 mg/m^2. SAMs with 100% C11OH resulted in the lowest HFG adsorption. The concentration of HFG on this monolayer was 1.5 ± 0.3 mg/m^2. For mixed C11OH SAMs, HFG adsorption decreased from 5.2 ± 0.8 mg/m^2 (36% C11OH) to 3.5 ± 0.2 mg/m^2 (65% C11OH). It is clear that concentration of adsorbed HFG decreases linearly with

the increase of C11OH percentage on the SAMs surfaces. HFG adsorption onto gold substrate was 5.2 ± 0.6 mg/m^2.

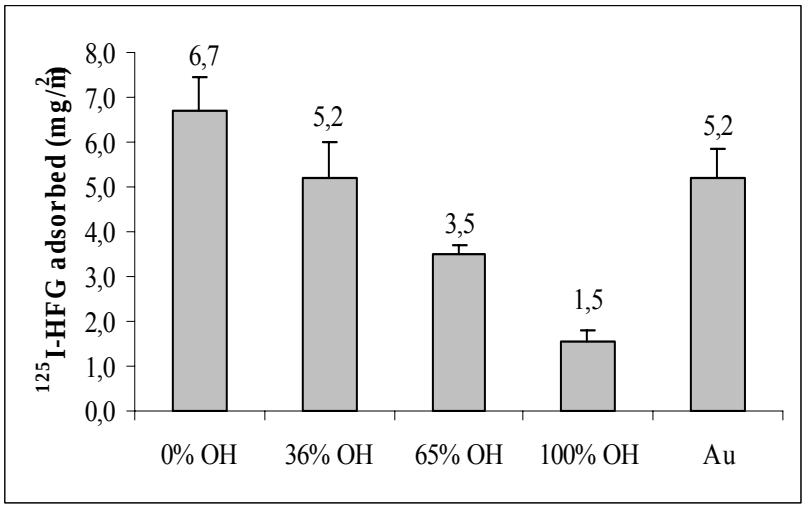

Figure 32. HFG adsorption on C11 SAMs using ^{125}I-HFG (0.1mg/ml; 25ºC; 30 min).

The theoretical monolayer coverage for HFG is 2.0 mg/m^2 for side-on orientation and 18 mg/m^2 for end-on orientation.[103] The results obtained suggest that, except for the OH-terminated SAM, all the surfaces could have protein monolayers with mixed side-on and end-on orientation.

3.2.3.2. Exchangeability of adsorption

The exchange of the pre-adsorbed ^{125}I-labelled HFG by other proteins in solution (HSA and HFG) was used in order to evaluate exchangeability of HFG adsorption onto different SAMs. Figure 33 shows the HFG retention onto the different SAMs, after being wet over a 24 hour period in HFG and HSA solutions (1mg/mL). The retention of the ^{125}I-labeled HFG after being wet in unlabeled HFG is lower only in hydrophilic SAM (100% of C11OH). When SAMs are wet in HSA solution, the retention of ^{125}I-labelled HFG was higher in almost all the

SAMs except that with 65% of C11OH. Thus, for the SAMs with 65% of C11OH, the pre-adsorbed HFG was exchanged more by HSA (± 40%) than by HFG.

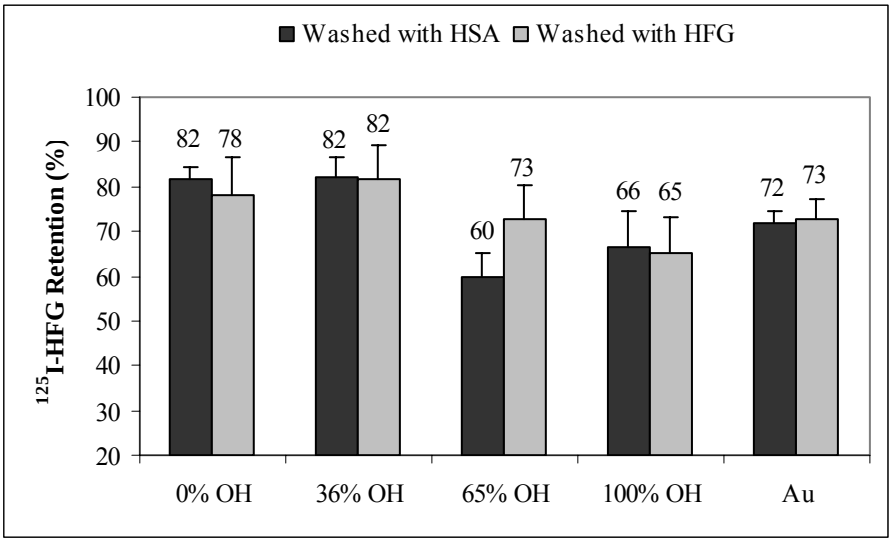

Figure 33. Retention of ^{125}I-HFG previously adsorbed to different SAMs prepared, after being washed with unlabelled HFG and HSA solution (1mg/ml; 25ºC; 24 h)

Gold substrates show almost the same surface retention for both solutions (HFG, 73± 4 % and HSA, 72± 3 %).

The more hydrophobic mixed SAMs with 0% and 36% C11OH present the highest HFG retention for both solutions (HFG, 78 ± 9 % and 82 ± 8 % and HSA, 82 ± 3 % and 82 ± 5 % respectively).

3.2.3.3. Competitive adsorption of HFG and HSA to SAMs

Competitive adsorption of HFG and HSA to different SAMs prepared from pure and a mixture of C11OH and C15CH3 was studied. Figure 34 shows the effect of the presence of unlabelled HSA on the adsorption of HFG onto SAMs with various C11OH concentrations.

The concentration of ^{125}I-labelled HFG was kept at 0.1mg/mL and the quantity of HSA was 0, 0.1 and 1mg/mL. Three replicates were used.

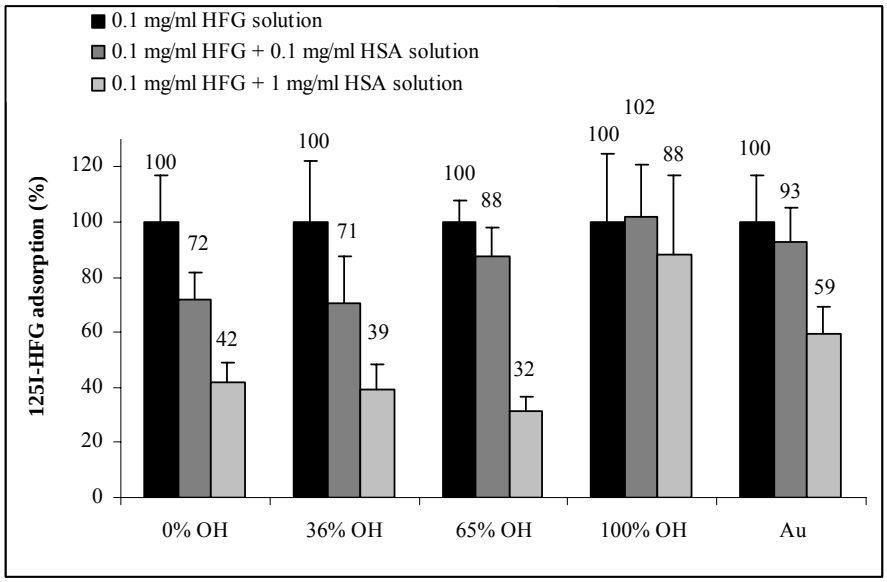

Figure 34. Competitive adsorption of HFG and HSA to different SAMs adsorbed from pure and acmixture of C11OH and C15CH3. The concentration of ^{125}I-labelled HFG was kept at 0.1mg/mL and the quantity of HSA was 0, 0.1 and 1mg/mL.

Calculations were performed considering that 100% adsorption corresponds to the concentration of HFG adsorbed from HSA-free solution (presented in Figure 30). Figure 32 shows the effect of the presence of albumin on fibrinogen adsorption.

When using the same concentration of fibrinogen and albumin (0.1/0.1mg/ml), the maximum decrease of fibrinogen adsorption was 30%, meaning that all the SAMs used seemed to have higher affinity to fibrinogen than to albumin,

For protein concentration in the same ratio of blood, some differences can be observed. The more hydrophobic surfaces (0%, 36% and 65% C11OH) showed the lowest affinity to fibrinogen. In 65% C11OH SAM, the presence of albumin lead to a decrease of fibrinogen adsorption of 70%. In opposition, it is clear that hydrophilic SAMs (100% C11OH) are the

surfaces that present higher affinity for fibrinogen, since they showed the lowest decrease of fibrinogen adsorption (12%) in the presence of albumin.

These results suggest that although surfaces with 100% C11OH present the lowest fibrinogen adsorption from pure solutions, when albumin was present as competitive protein, this surface had the highest fibrinogen affinity.

Competitive adsorption studies demonstrate that the more hydrophobic SAMs (0%, 36% and 65% C11OH) have higher affinity to HSA than the most hydrophilic SAMs (100% C11OH) and gold surfaces. However, SAMs with 0% and 36% C11OH, present the highest retention of HFG (Figure 33), showing that protein could be denaturated on the surface. The change of HFG conformation due to adsorption, could be related with platelet adhesion and activation. Therefore, SAMs with 65% C11OH, seemed to be the surface with the highest albumin affinity related with the lowest retention, suggesting that adsorbed HFG is on his native conformation.

3.2.3.4. Platelet adhesion and activation to SAMs and gold substrate

i. Scanning Electron Microscopy (SEM)

Figure 35 shows typical scanning electron micrographs of adherent platelets from the same donor on four different SAMs (0%, 36%, 65%, and 100% OH) and the Au control after pre-immersion in albumin solution or PBS. The platelet adherent density was analysed on randomized full-scale x-1000 images. With exception for SAMs with 65% OH, where platelet adhesion was not observed, results demonstrated an increase of the amount of platelet adhesion as the methyl groups on the surface increased. Platelet adhesion was also high on gold.

Comparing images of pre-immersed samples in PBS with pre-immersed samples in albumin solution, it is clear that the albumin layer inhibits platelet adhesion in all SAMs analysed.

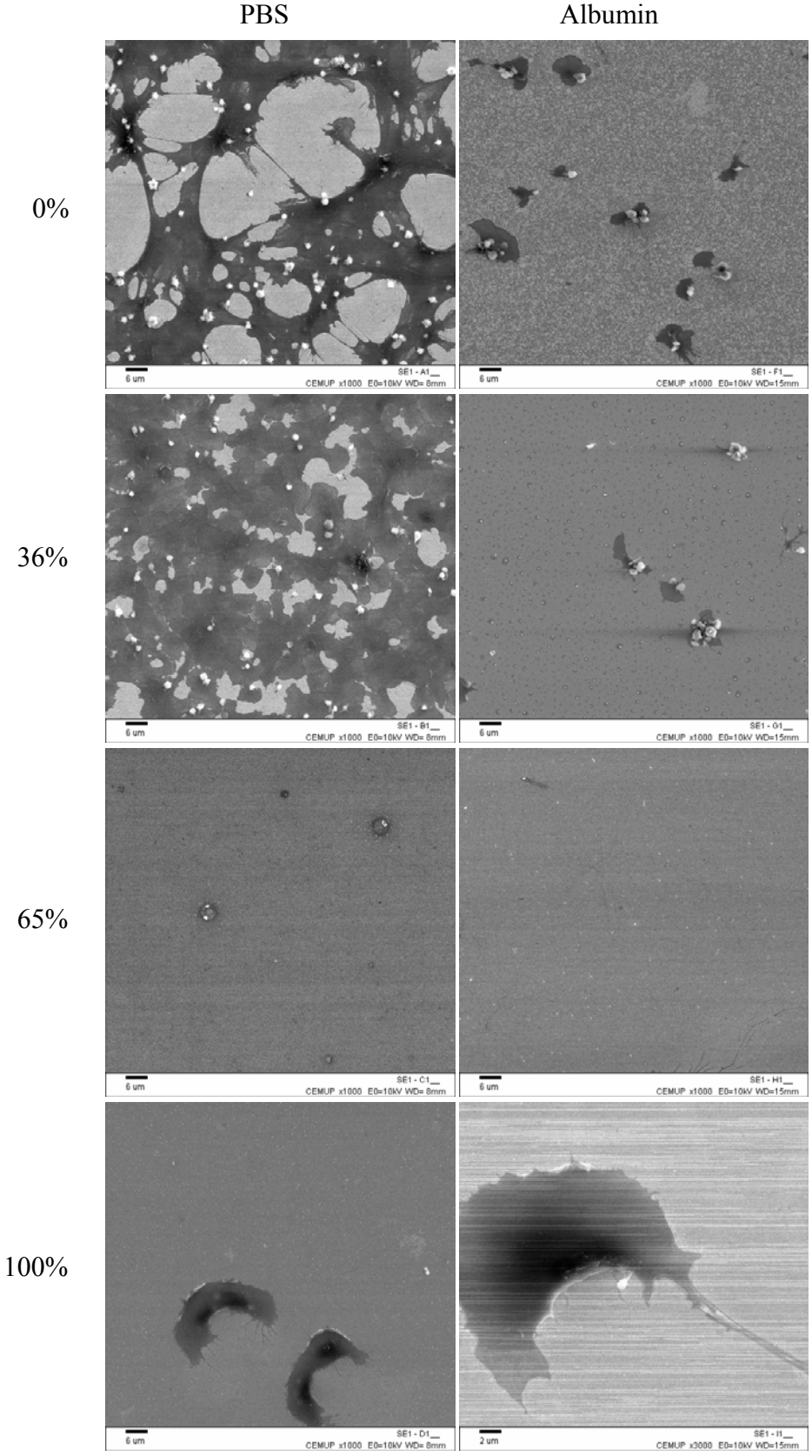

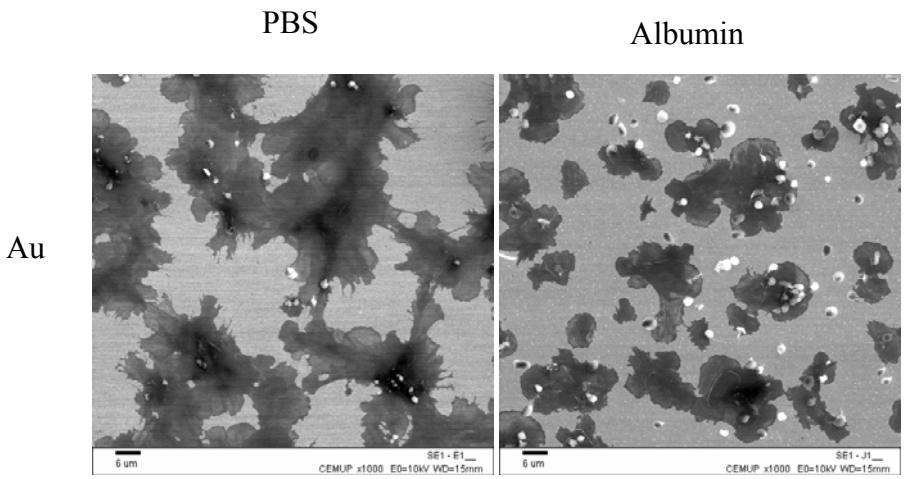

Figure 35. SEM micrographs of platelet adhesion on SAMs; O% OH; 36% OH; 65% OH; 100 % OH; and Au; all in PBS and in protein respectively.

These images are in accordance with the ones described by other authors for -OH and -CH_3 terminated SAMs and gold.[116-118]

Once the PRP used in these experiments had some proteins, results can be related with our previous protein adsorption studies, since the amount and denaturation of HFG is related with platelet adhesion and activation.[71] Higher platelet adhesion was observed on 0%, 36% SAMs and gold surfaces, which were the surfaces that demonstrate higher HFG adsorption and retention (higher HFG denaturation). Platelet adhesion was absent from 65% C11OH SAMs in both pre-immersion solutions (PBS and HSA). This surface presented the lowest affinity to HFG in the presence of HSA, as previously stated by us and the higher affinity to HSA in the presence of HFG as described by other authors.[1] Although 100% C11OH SAMs have the lowest protein adsorption, they presented some spread platelet on the surface, perhaps due to its higher fibrinogen affinity. This can also be observed in the surfaces that were pre-immersed in albumin solution.

In Figure 36 it can be observed some examples of the platelet adherent density analysed on randomized full-scale x-5000 images, where it is possible to distinguish different shapes and stages of platelet activation.

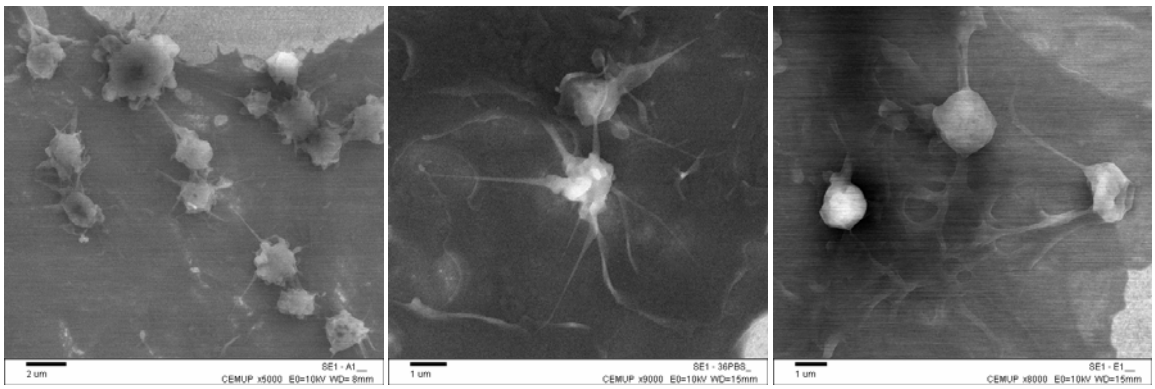

Figure 36. SEM micrographs of platelet adherent density was analysed on randomized full-scale x-5000 images on SAMs: 0% OH, 36% OH and Au, respectively, all pre-immersed in PBS solution.

Lin et al[116] described that on untreated Au surface, some adherent platelets were activated and the platelet shape was changed from round type (nonactivated) to dendritic or spread-dendritic type with few pseudopods extruded, and even fully spread type.

The hydrophobic -CH3 SAM was highly platelet reactive because the shape of the adhered platelet was mostly in spread dendritic and spread forms. For the hydrophilic -OH SAM surface, only few platelets adhered.[116]

ii. Glutaraldehyde Induced Fluorescence Technique – GIFT

Frank et al.[120] described this method as rapid, simple, and inexpensive for the investigation of platelet/material interactions, which allows imaging and quantification of adherent and spread platelets in parallel. The GIFT technique is stable without relevant photo bleaching. The fixed

samples can be stored for months and reinvestigated several times without affecting the image quality.[119] GIFT can be used to image the platelet shape change on foreign surfaces.

In this study, preliminary results were achieved regarding gold surfaces to evaluate platelet adhesion. Two PRP concentrations were used and a control surface without incubation in PRP concentrate was used.

Figure 37 illustrates that GIFT can be used to differentiate between the various categories of platelets shape. Different shapes are evident in these images, and it is shown that GIFT can be used as a tool to quantify adherent platelets. The GIFT technique results in high-contast images.

In the future, this technique will be used to quantification and qualification of platelet adhesion onto SAMs.

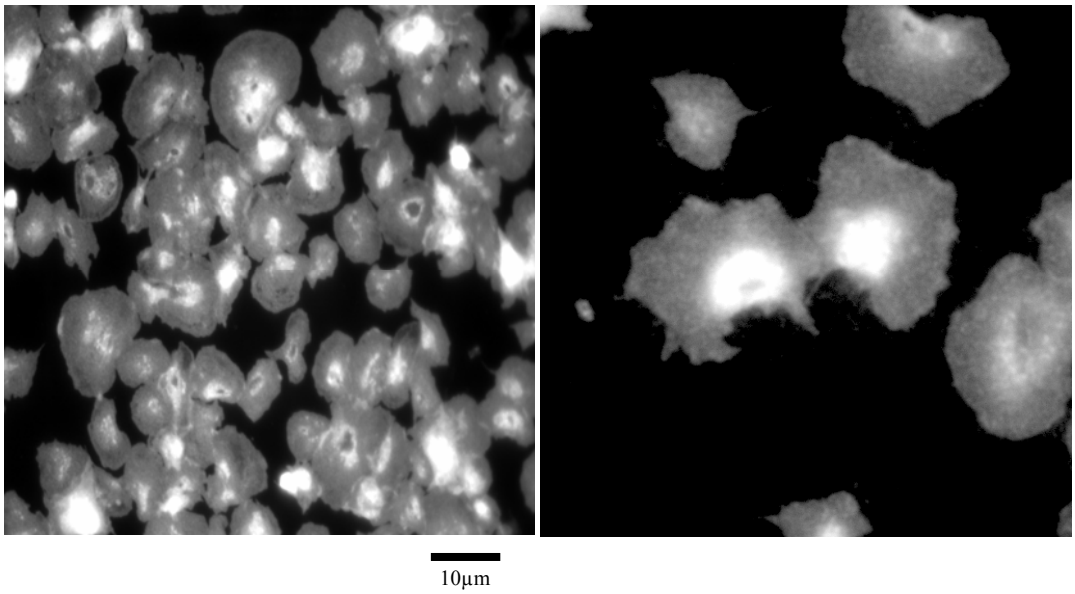

Figure 37. Representative GIFT images of adherent platelets on gold surfaces: left image obtained with concentration A (3 x 10^8 PLT/ml); right image obtained with concentration B (1.5 x 10^8 PLT/ml).

Although platelets adhered to gold, with the lower platelet concentration significantly less adhered platelets. The adherent platelets remained in spreading form and spread dendritic

form, while in higher concentration platelets are in fully spread form. The level of platelet adhesion on gold is very high.

iii. Flow cytometry – FC

Flow cytometry can provide both quantitative (percentage of activated platelets) and qualitative (activation degree) information. Initial concentration (Ai, 3 x 10^8 PLT/ml) was measured before contact with surfaces. Three methods of sample preparation were applied as described in Table V in order to optimize the quantification of adherent platelets onto gold surfaces. The adsorbed platelets are the initial minus the ones measured in the supernatant that was in contact with the surface.

Table V. Methods of sample preparation for flow cytometry analyses. Different bottom materials and wall materials were used in order to evaluate platelet activation.

	Bottom	**Wall**
Au	Gold	Silicon
CV	Polystyrene	Polystyrene
CO	Gold	Polystyrene

In Figure 38 it can be observed that thrombin increase platelet activation. Comparing the different approaches of samples preparations it seems that gold sample attached to Silastic™ tubing is the sample with the lowest adhered platelets, since the platelet adhered are the initial platelet concentration (Ai) minus platelet concentration after contact with gold (AuA).

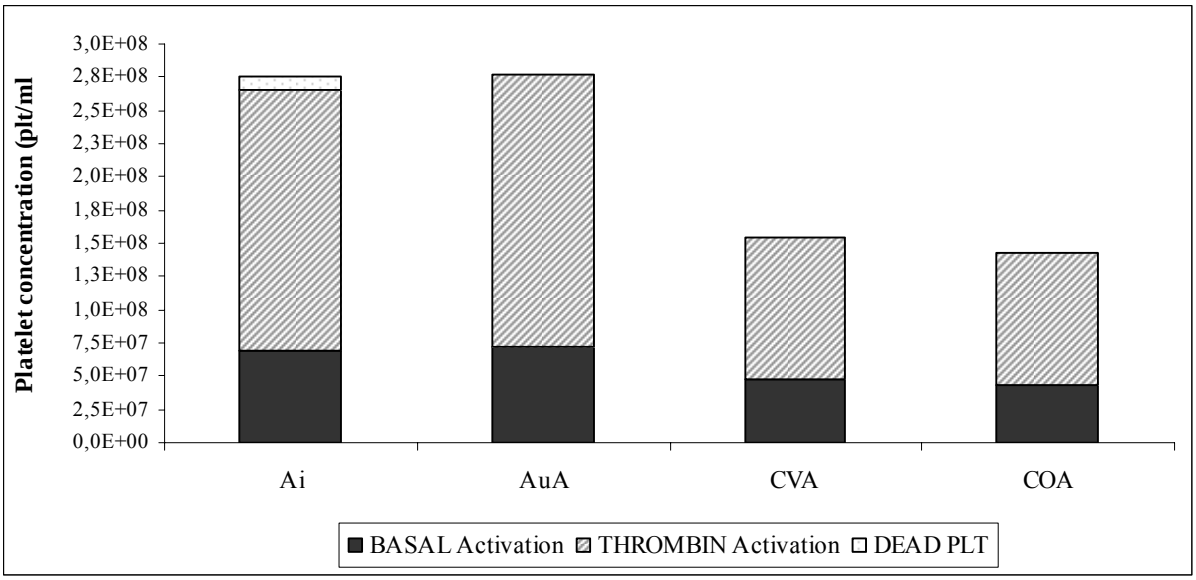

Figure 38. Platelet concentration of different samples and different typed of activation (basal and thrombin activation). Platelet concentration A (3 x 10^8 PLT/ml) was used.

Several authors have described that silicone is advantageous for long term extracorporeal respiratory support in terms of less platelet adhesion.[120] Davies et al also used Silastic™ tubing to attach cpTi test disks in order to evaluate platelet adhesion and platelet activation.[118]

4. Conclusions and perspectives

Ozonation of PET promoted a significant increase in hydrophilicity as evaluated by the decreasing of contact angle from 74º to 38.2º. The adhesion between PET and PHEMA was thus improved, as shown by tensile strength tests. Washed films presented higher contact angle as compared to unwashed films.

SEM micrographs confirmed that the best adhesion between treated PET fiber and PHEMA hydrogel matrix was obtained when PET fibers were treated with ozone for 6 hours and immediately immersed in a PHEMA reactive solution.

Tensile strength tests show that higher maximum stress can be obtained when PHEMA hydrogels are reinforced with PET fibers. Furthermore, the ozonation of PET fibers do not increase the maximum stress as compared to untreated ones. The behaviour of PHEMA hydrogels with untreated or ozone-treated PET fibers during tensile tests is significantly different. The maximum stress for PHEMA hydrogel without any reinforcement is ~0.09MPa and the maximum stress of ozonated bundles is ~11.6 MPa. Reinforcing the hydrogel with PET bundles modified by ozonation it is possible to obtain a maximum stress of ~0.34 MPa showing an increasing of mechanical properties of the composite.

Using pure and mixed SAMs prepared from solutions with only two different functional groups: OH-terminated thiol and CH3-terminated thiols it is possible to obtain a range of wettabilities.

Fibrinogen adsorption is lower on more hydrophilic surfaces as detected by protein radiolabelling. It is clear that the concentration of adsorbed HFG decreases linearly with the increase of C11OH percentage on the SAMs surfaces. Mixed SAMs (65% C11OH) show considerable HFG adsorption. This SAMs can be exchanged by albumin in solution, but they cannot be exchanged by fibrinogen in solution.

Although the more hydrophilic surface (100% C11OH) showed the lowest fibrinogen adsorption from pure solution, these surfaces demonstrated to have higher affinity for fibrinogen adsorption in the presence of albumin.

SEM micrographs showed that platelet adhesion was absent for 65% OH SAMs, which present the lowest affinity to HFG, as previously described.

With exception for SAMs with 65% OH, results demonstrated an increase of the amount of platelet adhesion as the methyl groups on the surface increased. Platelet adhesion was also high on gold.

The hydrophobic –CH3 SAM was highly platelet reactive because the shape of the adhered platelet was mostly in spread dendritic and spread forms, indicating that the contents of these activated platelets may have moved outward, causing more platelet adhesion and activation on the surface.

GIFT can be used to differentiate between the various categories of platelets shape. In the future, this technique will be used to quantification and qualification of platelet adhesion onto SAMs.

Flow cytometry will be used in order to quantify adhered platelets onto SAMs and evaluate their activation degree. This technique will be applied using SAMs attached to Silastic^{TM} tubing since it was the sample with the lower concentration of adhered platelets.

5. References

1. Martins MCL, Ratner BD, Barbosa MA. Protein adsorption on mixtures of hydroxyl- and methyl- terminated alkanethiols self-assembled monolayers.
2. Williams DF. The Williams dictionary of biomaterials. Liverpool University Press. 1999.
3. Ratner BD, Johnston A.B, Lenk TJ. Biomaterial surfaces, Journal of Biomedical Materials Research: Applied Biomaterials 1987; 21: 59-90.
4. Ratner, BD. Biomaterial sciences: An interdisciplinary endeavor. In: Ratner BD, Hoffman AS, Schoen FJ, Lemons JE, editors. Biomaterials Science. An Introduction to Materials in Medicine. California, USA: Academic Press 1996. 1-8.
5. Park JB. Biomaterials. In: Bronzino JD, editor. The Biomedical Engineering Handbook. Boca Raton, USA: CRC Press 1995. 530-536.
6. Galletti PM. Prostheses and artificial organs. In: Bronzino JD, editor. The Biomedical Engineering Handbook. Boca Raton, USA: CRC Press 1995. 1827-1837.
7. Ratner BD. New ideas in biomaterials science – a path to engineered biomaterials. J Biomed Mater Res 1993; 27:837-850.
8. Hench LL. Bioactive materials: The potencial for tissue regeneration. J Biomed Mater Res 1998; 41:511-517.
9. Ducheyne P, Bianco P, Radin S, Schepers E. bioactive materials: Mechanisms and bioengineering considerations. In: Ducheyne P, Kotubo T, van Blitterswijk CA, editors. Bone-Bonding. USA: Reed Healthcare 1992. 1-12.
10. Hench LL, Wilson J. Surface-active biomaterials. Science 1984; 226:630-636.
11. von Recum HA, Yaszemski MJ, Mikos AG. Tissue engineering concepts. In: Handbook of Biomaterials Evaluation: Scientific, Technical and Clinical Testing of Implant Materials, 2nd Ed. Ann Arbor, USA: Edwards Brothers 1999. 385-409.

12. Barenberg SA. Abridge report of the communittee to survey the needs and opportunities for the biomaterials industry. J Biomed Mater Res 1988; 22:1267-1291.

13. Aguilar MR, Rodriguez G, Fernández M, Gallardo A, Roman JS. Polymeric active coatings with functionality in vascular applications. J Mater Sci: Mater in Med 2002; 13: 1099-1104.

14. Patrick CW Jr, Mikos AG, McIntire LV. Prospectus of tissue engineering. In: Patrick CW Jr, Mikos AG, McIntire LV, editors. Frontiers in Tissue Engineering. Oxford, UK: Elsevier 1998.3-11.

15. Anderson JM. Biocompatibility of tissue engineered implants. Idem. 152-165.

16. Christenson L, Mikos AG, Gibbons DF, Picciolo GL. Biomaterials for tissue engineering: Summary. Tissue Eng 1997. 3:71-76.

17. Durfor CN. Biotechnology biomaterials: A global regulatory perspective of tissue-engineered products- Summary report and future directions. Tissue Eng 1997; 3:115-120.

18. Osmtead DR, Baird LG, Christenson L., Du Molin G, Tubo R, Maxted DD, Davis J, Gentile FT. voluntary guidance for the development of tissue-engineered products. Tissue Eng 1997; 3:239-266.

19. Piskin E. Biomaterials in different forms for tissue engineering: An overview. In: Liu D-M, Dixit V, editors. Porous Materials for Tissue Engineering, Materials Science Forum, vol 250. Uetikon-Zuerich Switerzland: trnas Tech 1997. 1-14.

20. Biomaterials Research in the 1990s. An Interview with Jack Lemons. Med Dev Diag Indust 1996; sept: 44.

21. Mooney DJ, Langer RS. Engineering biomaterials for tissue engineering : The 10-100 micro size scale.In: Bronzino JD, editor. The Biomedical Engineering Handbook. Boca raton, USA:CRC Press 1995. 1609-1618.

22. Galletti PM, Aebischer P, Lysaght MJ. The dawn of biotechnology in artificial organs. ASAIO J 1995; 41:49-57.

23. Peppas NA, Langer R. New challenges in biomaterials. Science 1994; 263:1715-1720.

24. Bell E. Biotechnology meets biomaterials. J Cell Biochem 1994; 56:147-149.

25. Hellman KB, Picciolo GL, Fox CF. Biotechnology applications in biomaterials. J Cell Biochem 1994;56:143-144.

26. Rudolph AS. Biomaterial biotechnology using self assembled lipid microstructures. J Cell Biochem 1994; 56:183-187.

27. Ringsdorf H. From molecules, macromolecules and supramolecular systems. Supramol Sci 1994; 1:5-6.

28. Reddi AH. Symbiosis of biotechnology and biomaterials: Applications in tissue engineering of bone and cartilage. J Cell Biochem 1994; 56:192-195.

29. Lazzeri L. Progress in bioartificial polymeric materials. Trip 1994; 4:249-252.

30. Piskin E. Biologically modified polymeric material surfaces: Introduction. Clin Mater 1992; 11:3-7.

31. Hoffman AS. Present and emerging applications of polymeric biomaterials. Clin Mater 1992; 11:13-18.

32. Andrade JD. Needs, problems and opportunities in biomaterials and biocompatibility. Clin Mater 1992; 11:19-23.

33. Hoffman AS. Immobilization of biomolecules and cells on and within polymeric materials. Clin Mater 1992; 11:61-66.

34. Spector M. Biomaterials : Taming the beast. J Biomed Mater Res 1992; 26:1-5.

35. Barenberg SA. Report of the committee to survey the needs and opportunities for the biomaterials industry. MRS Bull 1991; Sept:26-32.

36. Kohn J. Current trends in the development of synthetic materials for medical applications. Med Dev Technol 1990; Nov/Dec: 34-38.

37. Sun S, Yue Y, Huang X, Meng D. Protein adsorption on blood contact membranes. J Membrane Sci 2003; 222: 3-18.

38. Barenberg SA. Abridged report of the committee to survey the needs and opportunities for the biomaterials industry. J Biomed Mater Res 1988; 22:1267-1291.

39. Feng L, Andrade JD. Protein adsorption on low temperature isotropic carbon. I.Protein conformational change probed by differential scanning calorimetry. J Biomed Res. 1994; 28:735.

40. Williams DF. Definitions in Biomaterials, progress in Biomedical Engineering 4, Elsevier, Amsterdam, 1987.

41. Hoffman AS. Biologically functional materials. In: Ratner BD, Hoffman AS, Schoen FJ, lemons JF, editors. Biomaterials Science-An Introduction to Materials in Medicine. California, USA: Academic Press1996. 124-130.

42. Hasirci VN. Immobilization of biological active species. In: Muster D, editor. Biomaterials – Hard Tissue Repair and Replacement. Amsterdam, The Netherlands: Elsevier; 1998. 121-137.

43. Gorbet MB, Sefton MV. Biomaterial-associated thrombosis: roles of coagulation factors, complement, platelets and leukocytes. Biomaterials, 2004

44. Okano T,Yamada N, okuhara M, Sakai H, Sakurai Y. Mechanism of cell detachment from temperature modulated, hydrophilic-hydrophobic surfaces. Biomaterials 1995; 16: 297-304.

45. Vogler EA. Biomaterial sciences: The role of water in Biomaterials. In: Ratner BD, Hoffman AS, Schoen FJ, Lemons JE, editors. Biomaterials Science. An Introduction to Materials in Medicine. 2nd Edition. Elsevier Academic Press 2004. 59-61.

46. Andrade JD and Hlady V. Protein adsorption and materials biocompatibility: a tutorial review and suggested hypotheses. Advances in Polymer Science 1986; 79:1-63.

47. Norde W. Adsorption of proteins from solution at the solid-liquid interface. Advances in Colloid and Interface Science 1986; 25:267-340.

48. Dent AH and Aslam M. Other categories of protein coupling in: Bioconjugation, protein coupling techniques for the biomedical sciences, edited by Aslam M and Dent AH. Macmillan reference Ltd. London1998:504-569.

49. Van Oss CJ. Hydrophobicity and hydrophilicity of biosurfaces. Current Opinion in Colloid and Interface Science 1997; 2:503-512.

50. Ratner BD. Biomaterial sciences: The role of adsorbed protein s in tissue response to biomaterials. In: Ratner BD, Hoffman AS, Schoen FJ, Lemons JE, editors. Biomaterials Science. An Introduction to Materials in Medicine. 2nd Edition. Elsevier Academic Press 2004. 237-246.

51. Chinn JA. Biomaterials: Protein-Surface Interactions in The Biomedical Engineering Handbook; edited by Bronzino JD. CRC Press. USA 1995:1597-1608.

52. Stryer L. Biochemistry. 4th ed, WH Freeman, New York. 1998.

53. Branden C and Tooze J. Introduction to Protein Structure. 2th ed. Published by Garland Publishing, Inc.USA.1999.

54. Lee JH, Kim HW, Pak PK, Kim SS and Lee HB. Protein behavior on polymer surfaces with hydrophilic functional groups. Korea Polymer J. 1994; 2:32-39.

55. Nakanishi K, Sakiyama T and Imamura K. On the adsorption of proteins on solid surfaces, a common but very complicated phenomenon. J Bioscience and Bioengineering 2001; 91:233-244.

56. Brash JL. Studies of protein adsorption relevant to blood compatible materials, in Modern Aspects of Protein Adsorption on Biomaterials, edited by Missirlis YF and Lemm W. Kluwer academic Publishers, The Netherland 1991; 38-47.

57. Hlady V and Buijs J. Protein adsorption on solid surfaces. Current Opinion in Biotechnology 1996; 7:72-77.

58. Norde W and Lyklema J. The adsorption of human plasma albumin and bovine pancreas ribonuclease at negatively charged polystyrene surfaces. I Adsorption isoterms. Effects of charge, ionic strength and temperature. J Colloid Interface Science 1978; 66:257-265.

59. Dulm PV and Norde W. The adsorption of human plasma albumin on solid surfaces, with special attention to the kinetics aspects. J Colloid Interface Science 1883; 91:248-255.

60. Haynes CA, Sliwinsky E and Norde W. Structural and electrostatic properties of globular proteins at a polystyrene-water interface. J Colloid Interface Sci. 1994; 164:394-409.

61. Stryer L. Biochemistry. 4th ed, WH Freeman, New York. 1998.

62. Lee JH, Lee HB and Andrade JD. Blood compatibility of polyethylene oxide surfaces. Prog. Poly Sci. 1995; 20:1043-1079.

63. Dailey JF. Blood. 2th ed. Published by Medical Consulting Group. Ipswich, MA, USA.1998.

64. Sigal GB, Mrksich M and Whitesides GM. Effect of surface wettability on the adsorption of proteins and detergents. J. Am. Chem. Soc. 1998; 120:3464-3473.

65. Yee VC, Pratt KT, Cole HCF, Le Trong I, Chung DW, Davie EW, Stenkamp RE and Teller DC. Crystal structure of a 30 kDa C-terminal fragment from the γchain of human fibrinogen. Structure. 1997; 5(1): 125-138.

66. Peters T Jr. All about albumin: biochemistry, genetics and medical applications, Academic Press, Inc., San Diego, CA. 1996.

67. Carter DC, He XM, Munson SH, Twigg PD, Gernert KM, Broom MB and Miller TY. Three-dimensional structure of human serum albumin. Science. 1989; 244:1195-1198.

68. Muller M, Werner C, Grundke K, Eichhorn KJ and Jacobasch HJ. Spectroscopic and thermodynamic characterizationof the adsorption of plasma proteins onto cellulosic substrates. Macromol Symp. 1996; 103:55-72.

69. Sergio S, Kashina A, Mochizuki S, Noda M and Kabayashi K. Crystal structure of serum albumin at 2.5 Å resolution. 1999; 12 (6): 439-446.

70. Minghetti PP, Ruffner DZ, Kuang WJ, Dennison OZ, Hawkins JW, Beattie WG and Dug A. J. Biol. Chem. 1986; 15: 6747-6757.

71. Ratner BD. Biomaterial sciences: the complement system. In: Ratner BD, Hoffman AS, Schoen FJ, Lemons JE, editors. Biomaterials Science. An Introduction to Materials in Medicine. 2nd Edition. Elsevier Academic Press 2004. 318-338.

72. Chandy T, Mooradian DL and RaoGHR. Platelet adhesion and spreading on protein coated surfaces: variations in behaviour in washed cells, PRP and Whole blood. J Biomaterials Applications 1998; 13:46-65.

73. Savage B and Ruggeri ZM. Selective recognition of adhesive sites in surface-bound fibrinogen by glycoprotein IIb-IIIa on nonactivated platelets. J Biol Chem. 1991; 266:11227-11233.

74. Difazio LT, Stratoulias C, Greco RS and Haimovich B. Multiple platelet surface receptors mediate platelet adhesion to surfaces coated with plasma proteins. J Surgical Res. 1994; 57:133-137.

75. Goodman SL. Sheep, pig, and human platelet-material interactions with model cardiovascular biomaterials. J Biomed Mater Res 1999; 45(3): 240-250.

76. Bain CD, Troughton EB, Tao YT, Evall j, Whitesides GM and Nuzzo RG. Formation of monolayer films by spontaneous assembly of organic thiols from solution onto gold. J Am Chem Soc. 1989; 111:321-335.

77. Ulman A. Formation and structure of self-assembled monolayers. Chemical Reviews. 1996; 96:1533-1554.

78. Ulman A. Self-Assembled Monolayers, in An Introduction to Ultrathin Organic Films. Academic Press Inc., San Diego, CA, USA, 1991. 237-304.

79. Prime KL and Whitesides GM. Adsorption of proteins onto surfaces contain end-attached oligo(ethylene oxide): A model systems using self-assembles monolayers. J Am Chem Soc, 1993; 115: 10714-10721.

80. Prime KL and Whitesides GM. Self-assembled organic monolayers: model systems for studying adsorption of proteins at surfaces. Science1991; 252:1164-1167.

81. Lopez GP, Albers MW, Schreiber SL, Carrol R, Peralta EE, Whitesides GM. Convenient methods of patterning the adhesion of mammalian-cells to surfaces using self-assembled monolayers of alkanethiolates on gold. J Am Chem Soc, 1993; 115: 5877-5878.

82. Deng L, Mrksich M, Whitesides GM. Self-assembled monolayers of alkanethiolates presenting tri(propylene sulfoxide) groups resist the adsorption of protein. J Am Chem Soc 1996; 118: 5136-5137.

83. Patel N, Davies MC, Hartshorne M, Heaton RJ, Roberts CJ, Tendler SJB, Williams PM. Immobilization of protein molecules onto homogeneous and mixed carboxylate-terminated self-assembled monolayers. Langmuir 1997; 185: 94-103.

84. Cotton C, Glidle A, Beamson G, Cooper JM. Dynamics of the formation of mixed alkanethiols monolayers (SAMs). Langmuir 1998; 14: 5139-5146.

85. Lindbad M, Lestelius M, Johansson A, Tengvall P, Thomsen P. Cell and soft tissue interactions with methyl- and hydroxyl-terminated alkane thiols on gold surfaces. Biomaterials; 1997; 18: 1059-1068.

86. Iannace S, Sabatini G, Ambrosio L, Nicolais L. Mechanical behaviour of composite artificial tendons and ligaments. Biomaterials 1995; 16, N.9. ISSN: 0142-9612.

87. Ambrosio L, Netti PA, Iannace S, Huang SJ, Nicolais L. Composite hydrogels for intervertebral disc prostheses. Journal of Materials Science: Materials in Medicine, 1996. 7, 251-254, ISSN: 0957-4530.

88. Ambrosio L, Iannace S, Netti PA, De Santis R, Nicolais L. Viscoelastic behavior of composite ligament prostheses. Journal of Biomedical Materials Research 1998; Vol. 42, 6-12.

89. Karlsson J, Michalec J, Gatenholm P. Surface characterisation of fiber supported hydrogels. In: Surface Modification of Polymeric Biomaterials, edited by B.D.Ratner and D.G.Castner, Plenum Press, New York 1996; 79-87.

90. Walzak MJ, Flynn S, Foerch R, Hill JM, Karbashewski E, Un A, Strobel M. UVand ozone treatment of polypropylene and poly(ethylene terephtalate). Journal of Adhesion Science Technol. 1995; 9:1229-1248.

91. Mcintyre NS and Walzak MJ. New UV/Ozone treatment improves adhesiveness of polymer surfaces. Modern Plastics. 1995; 79-83.

92. Hill JM, Karbashewski E, Un A, Strobel M, Walzak MJ. Effects of aging and washing on UV and ozone-treated poly(ethylene terephtalate) and polypropylene. Journal of Adhesion Science. Technol. 1995; 9:1575 -1591.

93. Pietro Favia, Fabio Palumbo, Marco Vito Stendardo, Riccardo d'Agostino. Plasma-treatments of polymers by NH3-H2 RF glow discharges: coupling plasma and surface

diagnostics. In: Surface Modification of Polymeric Biomaterials, edited by B.D.Ratner and D.G.Castner, Plenum Press, New York, 1996; 69-77.

94. Neil P. Desai and Jeffrey A. Hubell. Surface physical interpenetrating networks of polyethylene terephthalate and polyethylene oxide with biomedical applications. Macromolecules, Vo1.25, N° 1, 1992.

95. Neil P. Desai and Jeffrey A. Hubell. Biological responses to polyethylene oxide modified polyethylene terephthalate surfaces. Journal of Biomedical Materials Research 1991, vo1.25, 829-843.

96. Wendel H.S, Ziemer Gerhard. Coating techniques to improve the hemocompatibility of artificial devices used for extracorporeal circulation. European j cardio-thoracic Surgery 1999; 16: 342-350.

97. Hanson SR, Harker LA, Ratner BD, and Hoffman AS. In vivo evaluation of artificial surfaces with a nonhuman primate modelo f arterial thrombosis. J Lab Cli Med 1980. 95: 289-304.

98. Ratner BD. Surface modifications of polymers: chemical, biological and surface analytical challenges. Biosensors Bioelectron. 1995; 10:755-764.

99. Feng XD, Sun YH, Qiu KY. Reactive site and mechanism of graft copolymerization onto poly(ether urethane) with ceric ion as initiator. Macromolecules 1985; 18: 2105-2109.

100. Peluso G, Petillo O, Anderson JM, Ambrosio L, Nicolais L, Melone MAB, Eschbach FO, Huang SJ. The differential effects of poly(2-hydroxyethyl methacrylate) and poly(2-hydroxyethyl methacrylate/poly(caprolactone) polymers on cell proliferation and collagen synthesis by human lung fibroblasts. J Biomed Mater Res 1997; 34:327-336.

101. Gehanno V, Freitas PP, Veloso A, Ferreira J, Almeida B, Sousa JB, Kling A, Soares JC, Silva MF. Ion beam deposition of Mn-Ir spin valves. IEEE Trans Magn; 1999; 35: 4361-4367.

102. Sastry M. A note on the use of ellipsometry for studying self-assembled monolayers. Bulletin of Materials Science 2000; 23(3): 159-163.

103. Feng L and Andrade JD. Protein adsorption on low temperature isotropic carbon. III. Isoterms, competitivity, desorption and exchange of human albumin and fibrinogen. Biomaterials 1994; 15:323-333.

104. Lima J, Sousa SR, Ferreira A, Barbosa MA. Interactions between calcium, phosphate, and albumin on the surface of titanium. J Biomed Mater Res 2001; 55: 45-53.

105. Iodine-125, a Guide to radioiodination techniques. Amersham Life Science; 1993: 64.

106. Kuptsov GH, Zhizhin GN. In: Fourier transform raman and infrared spectro of polymers. Elsevier 1998, 155.

107. Beamson G and Briggs D. In: High Resolution XPS of Organic Polymers 1992; 174-175.

108. Nakayama Y, Takahashi K, Sasamoto T. ESCA analysis of photodegraded poly(ethylene terephthalate) film utilizing gas chemical modification. Surf. Interface Anal. 1996 ; 24 : 711-717.

109. Ralph S. Greco, M.D. In: Implantation Biology - The host response and Biomedical Devices, 1994; 34.

110. Weibull W. Journal of Applied Mechanics. 1951; 18; 293.

111. Pompo A, D'Amore A, Saiello S, Nicolais L, Acierno 0, Bianchi R, Vosa R. Statistical aspects of tensile strength of poly(ethylene terephtalate) fibres. Journal of Materials Science Letters. 1992; 11 :504-507.

112. Ishida T, Tsuneda S, Nishida N, Hara M, Sasabe H, Knoll W. Surface-conditioning effect of gold substrates on octadecanethiol self-assembled monolayer growth. Langmuir 1997; 13: 51-55.

113. Bain CD and Whitesides GM. Formation of monolayer coadsorption of thiols on gold: variation in the head group, tail group and solvent. J Am Chem Soc. 1988; 110:3665-3666.

114. Castner DG, Hinds K,Grainger DW. X-ray photoelectron spectroscopy sulphur 2p study of organic thiol and disulfide binding interactions with gold surfaces. Langmuir 1996; 12: 5083-5086.

115. Porter MD, Bright TB, Allara DL, Chidsey CED. Spontaneously organized molecular assemblies. 4. Structural characterization of n-alkyl thiol monolayers on gold by optical ellipsometry, infrared spectroscopy and electrochemistry. J Am Chem Soc 1987; 109: 3559-3468.

116. Steven L. Goodman. Sheep, pig, and human platelet-material interactions with model cardiovascular biomaterials. J Biomed Mater Res 1998; 45 (3): 240-250.

117. Lin JC, Chuang WH. Synthesis, surface characterization, and platelet reactivity evaluation for the self-assembled monolayer of alkanethiols with sulfonic acid functionality. J Biomed Mater Res 2000. 51: 413-423.

118. Park JY, Gemmell CH, Davies JE. Platelet interactions with titanium: modulation of platelet activity by surface topography. Biomaterials 2001; 22: 2671-2682.

119. Frank RD, dresbach H, Thelen H, sieberth HG. Glutardialdehyde induced fluorescence technique (GIFT): A new method for the imaging of platelet adhesion on biomaterials. J Biomed Mater Res 2000. 52: 374-381.

120. Niimi Y, Yamane S, Yamaji K, Tayama E, Sueoka A, Nose Y. Protein adsorption and platelet adhesion on the surface of an oxygenator membrane. ASAIO J. 1997; 43(5): M706-10.